Eco-evolutionary dynamics of nested Darwinian populations and the emergence of community-level heredity

Guilhem Doulcier[1,2], Amaury Lambert[3,4], Silvia De Monte [†2,5], and Paul B. Rainey [†1,5]

[1]École supérieure de physique et de chimie industrielle de la ville de Paris, PSL Research University, 10 rue Vauquelin, 75005, Paris, France
[2]Institut de biologie de l'École normale supérieure (IBENS), École normale supérieure, CNRS, INSERM, PSL University, 46 rue d'Ulm, 75005, Paris, France
[3]Sorbonne Université, 75005, Paris, France
[4]Collège de France, PSL University, 75005, Paris, France
[5]Max Planck Institute for Evolutionary Biology, Plön, Germany

November 4, 2019

Abstract

Chance interactions among microbial cells can generate new chemistries and functions, but exploitation requires establishment of communities that reliably recapitulate community-level phenotypes. Using mechanistic mathematical models, we show how simple manipulations to population structure can exogenously impose Darwinian-like properties on communities. Such imposition causes communities to participate directly in the process of evolution by natural selection and drives the evolution of cell-level interactions to the point where, despite underlying stochasticity, derived communities give rise to offspring communities that faithfully re-establish parental phenotype. The mechanism is akin to a developmental process (developmental correction) that arises from density dependent interactions among cells. Knowledge of ecological factors affecting evolution of developmental correction has implications for understanding the evolutionary origin of egalitarian transitions in individuality, symbioses, and for top-down engineering of microbial communities.

Thirty years ago, in an article arguing the importance of the "superorganism", Wilson and Sober expressed surprise that biologists had not recognised that communities — in the laboratory — "*could be treated as entities with heritable variation and selected accordingly*" (Wilson and Sober, 1989). That they might be treated as such stemmed from recognition that the eukaryotic cell is a tight-knit community of two once free-living microbes (Margulis,

†: Co-senior authors. For correspondance: demonte@biologie.ens.fr, paul.rainey@espci.fr.

1970), but also from observations in nature of social insect colonies (Wilson, 1985), cellular slime molds (Bonner, 1982; Buss, 1982), and especially of phoretic insect communities (Wilson and Knollenberg, 1987).

Phoretic insect communities comprise a focal organism — often an insect such as a beetle — that moves between patchily distributed ephemeral resources carrying with it a myriad of associated organisms, including mites, nematodes and microbes. Communities associated with each insect differ by virtue of the composite members, with the conceivable possibility that some associations may harm the carrier insect, while others may benefit the carrier. Given that the role of dispersal as somewhat analogous to a reproductive event, Wilson and Sober argued that selection at the level of insect communities was likely to trump within-community selection leading to communities "*becoming organised into an elaborate mutualistic network that protects the insect from its natural enemies, gathers food, and so on.*"

If this might happen in nature, then why might this not be realised even more potently in the laboratory? Indeed, the logic of Darwinism says it should. Provided there exists heritable variance in fitness at the level of communities, then communities will participate as units in the process of evolution by natural selection in their own right. In nature, the necessary conditions are likely rare (Goodnight and Stevens, 1997), but ecological circumstances can sometimes conspire to ensure that variation among communities is discrete, that communities replicate and that offspring communities show some resemblance to parental communities. Phoretic insect communities are an apparent case in point. In the laboratory, however, the experimenter can readily construct conditions that ensure communities and / or collectives of cells are units of selection in their own right (Johnson and Boerlijst, 2002; Day et al., 2011; Xie and Shou, 2018; Xie et al., 2019). A critical requirement is a birth-death process operating over a time scale longer than the doubling time of individual cells (Hammerschmidt et al., 2014; Rainey et al., 2017; Black et al., 2019).

Empirical proof that selection really can shape communities was provided by Swenson and colleagues who performed two studies in which artificial selection was imposed on microbial communities from soil (Swenson et al., 2000a,b). In the first they imposed selection for communities that affected plant growth. In the second they selected communities for ability to degrade the environmental pollutant 3-chloroaniline. In both instances communities at extreme values of community function were repeatedly propagated. In both studies a significant response was measured at the level of the community.

Although the finding was a surprise to many (Goodnight, 2000), it is consistent with expectations that communities / collectives of entities — no matter their identity — will participate in the process of evolution by natural selection provided communities are discrete, they replicate and that offspring communities resemble parental communities (Godfrey-Smith, 2009). Discreteness is conferred by simply compartmentalising communities via their placement in independent vessels. Replication is achieved by taking a sample of the selected communities with transfer to a new vessel. Heredity, however, is less tangible, especially in the Swenson experiments, where the selected communities were pooled before redistributing into fresh vessels. Nonetheless, intuition says that heredity becomes established through interactions (Wilson and Sober, 1989; Goodnight, 2000). Understanding the mechanistic bases of community-level heredity and its emergence motivates our study.

We begin by posing a thought experiment realisable via ever improving capacity to manipulate small volumes of liquid (Sackmann et al., 2014). Consider a millifluidic device that controls the composition of emulsions. Consider thousands of micro litre-sized droplets each harbouring communities comprised of two types of microbe that differ solely in the

colour of a fluorescent protein: one type encodes a red fluorescent protein and the other a blue fluorescent protein. Interest is in the evolution of communities that are of the colour purple (an equal ratio of red to blue cells). Within each droplet red and blue microbes replicate with growth rate and interaction rates being subject to evolutionary change. In the mean time the experimenter, via lasers installed on the device, has determined the precise colour of each droplet and *a priori* decided that half of the droplets furthest from an equal ratio of red-to-blue will be eliminated, whilst the fraction closest to the colour purple will be allowed to replicate. Replication involves a dilution step during which nutrients are replenished. A further round of growth then ensues along with a further round of droplet-level selection. The protocol continues thereafter with selection taking place at the level of communities maintained within droplets via a death-birth process. Figure 1 depicts the schema.

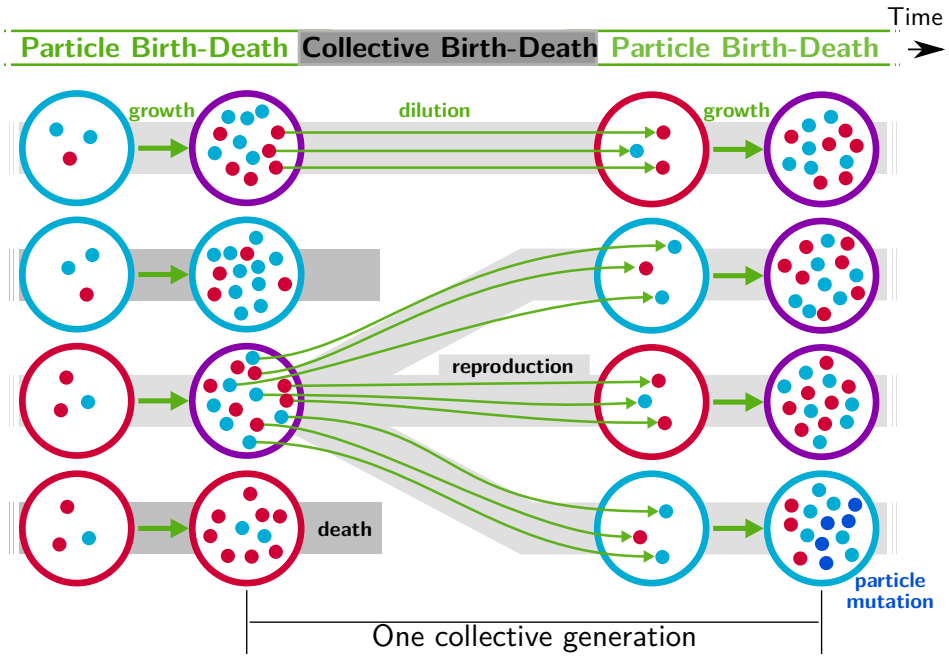

Figure 1: **Nested model of evolution**. Collectives (large circles) follow a birth-death process (grey) with non-overlapping generations. Collectives are composed of particles (small spheres) that also follow a birth-death process (*growth*, represented by thick green arrows). Offspring collectives are founded by sampling particles from parent collectives (*dilution*, represented by thin green arrows). Survival of collectives depends on colour. Collectives that contain too many blue or red particles are marked for extinction. The number of collectives is kept constant. Mutation affects particle traits (see main text for details).

Under this regime communities within droplets are endowed with Darwinian-like properties (we use this term to convey the fact that removal of the scaffold leads to, at least initially, complete loss of community-level individuality). Collective-level variation is discretised by virtue of the bounds provided by the immiscibility of oil and water (communities are thus confined to droplets). Additionally, the device ensures that droplets engage in a death-birth process: droplets furthest from the collective-level trait are extinguished, whereas those clos-

est to the colour purple are diluted and split thus effecting collective-level reproduction. Not determined by the device however is the relationship between parent and offspring droplets. Because the trait of the parent community depends on properties of the cellular constituents, there is — in the absence of interactions between red and blue cells — little chance that purple-coloured communities will reliably give rise to purple-coloured offspring. This is in part due to the stochastic nature of the dilution phase (a droplet with an equal ratio of red to blue is unlikely to give rise to offspring droplets founded with the same equal ratio of types) but also to within-droplet selection favouring fast growing types. Nonetheless, purple coloured droplets can in principle be maintained simply by imposing hard community-level selection in a manner envisioned by the "stochastic corrector" model (Maynard Smith and Szathmary, 1995; Grey et al., 1995; Johnston and Jones, 2015). But it is conceivable that repeated imposition of droplet level selection might lead to the evolution of interactions among the constituent cells akin to a developmental process. Such a process would ensure that the ratio of red to blue cells, no matter their ratio in newly "born" communities, would, after replication of cells and achievement of "adult" stage, resemble previous parental community phenotypes.

1 Results

1.1 A nested model of collective evolution

Our model, based on the schema outlined above and depicted in Figure 1, supposes a population of collectives subject to a birth-death process. Each collective is comprised of two kinds of self-replicating particles (red and blue) that together determine collective colour. Colour is important because it is the phenotype upon which collectives succeed or fail. Collectives that are too far from an optimal colour face extinction, whereas those within acceptable bounds persist with the possibility of reproduction. Birth-death at the level of collectives affects the eco-evolutionary dynamics of particles. We capture this scenario with a nested model and begin with numerical simulations of the stochastic, multi-level demographic process. In the next section an analytical approximation is presented.

In the numerical model (Appendix A), the ecological dynamic of particles is expressed by a stochastic birth-death process (Champagnat et al., 2006; Doebeli et al., 2017). Each particle of type $i \in \{0, 1\}$ is characterised by four traits (hereafter *particle traits*): colour (c_i, red or blue), net maximum growth rate r_i, and two competition parameters (a_i^{intra} and a_i^{inter}). At any particular instance particles either reproduce or die. Particles of type i reproduce with a constant birth rate r_i and die as a consequence of competition. The rate of death is density-dependent such that each particle of type j increases the death rate of i-type particles by $r_i a_j^{\text{intra}}$ if they share the same colour ($c_j = c_i$), or by $r_i a_j^{\text{inter}}$ when colours are different ($c_j \neq c_i$). All transition rates can be found in Appendix A Table A.4.

Mutations are introduced at the level of particles. Mutation affects either particle maximum growth rate (r) or the inter-colour competition parameter (a^{inter}) by a small random quantity. In the spirit of adaptive dynamics (Geritz et al., 1998), the particle type carrying the new set of traits is referred to as a mutant, and the existing type is designated the resident. Mutations are assumed to be rare. In order to accelerate numerical simulations one mutant type is introruced at every extinction event, with the the mutant bearing the same colour as the extinct type.

Collectives also undergo a birth-death process. The number of collectives D is constant and collective generations are discrete and non-overlapping. Each collective generation be-

gins at time $t = 0$ with offspring collectives containing B founding particles. Particles replicate, interact and evolve according to the particle traits. After duration T, collectives attain "adult" status, and a fixed proportion of collectives ρ is marked for extinction. This allows the possibility of selection on collectives based on their properties (collective phenotype), which is derived from the composing particles. Our focus is collective colour, which is defined as the proportion of red particles.

Initially, collectives contain red and blue particles in uniformly distributed ratios. Collectives are subject to evolution under two contrasting regimes: one neutral and the other selective. Under the neutral regime, the pool of collectives marked for extinction is sampled at random, whereas under the selective regime, collectives marked for extinction are those whose adult colour departs most from an arbitrarily fixed optimal colour. Extinguished collectives are replaced by offspring from uniformly sampled extant collectives (Figure 1). All other collectives are replaced by their own offspring. Reproduction involves uniformly sampling B particles from the parent collective. Particles from one collective never mix with particles from any other. This establishes an unambiguous parent-offspring relationship (De Monte and Rainey, 2014). The adult colour of offspring collectives depends on the founding frequencies of particles (whose variance is negatively related to bottleneck size B), and on ensuing particle-level population dynamics.

1.2 Selection on collectives drives the evolution of particle traits

In the absence of collective-level selection (neutral regime) collectives rapidly converge on a monochromatic phenotype (Figure 2A). Once collectives are composed of either all-red or all-blue particles, the contrasting colour cannot be rescued, since colour change by mutation or migration is not possible. The distribution of collective colour is thus quickly biased toward faster growing particle types with selection driving particle growth rate (Figure 2C). The inter-colour competition trait (Figure 2E) is irrelevant once collectives become monochromatic (it then evolves by random drift).

The dynamic is very different once selection is imposed at the level of collectives. By rewarding collectives closest to the colour purple (a fixed $\hat{\phi} = 0.5$ ratio of red to blue particles) it is possible to prevent fixation of either colour (Figure 2B). Starting, as above, from collectives containing red and blue particles in uniformly distributed ratios, mean collective colour shifts rapidly toward red as a consequence of the faster initial growth rate of red particles, but after a few tens of generations mean collective colour approaches purple. From generation 1,000, variance of the colour distribution progressively decreases. This is indicative of improvement in the ability of purple parent collectives to give rise to offspring collectives that resemble parental types. This is associated with escalating particle growth rate (Figure 2D) and a saturating increase in between-colour competition. The latter reflects directional selection that moves the population of collectives towards an optimal trait value (reached by generation 7,000 see Figure 2F).

By affecting particle parameters, selection on colour also modifies dynamics within collectives. Figure 3 shows variation of colour within a single collective generation: at generation 3 and generation $9,000$. Prior to selection shaping particle traits, both red and blue particle types follow approximately exponential growth (Figure 3C). The resulting adult collective colour is thus biased towards the faster growing red type. In contrast, at generation $9,000$ (Figure 3B), both particle types reach a saturating steady state that ensures that adult colour is purple. Initial departures from a 1:1 ratio – caused by the stochasticity of collective reproduction and / or particle growth dynamics – are compensated for during the latter

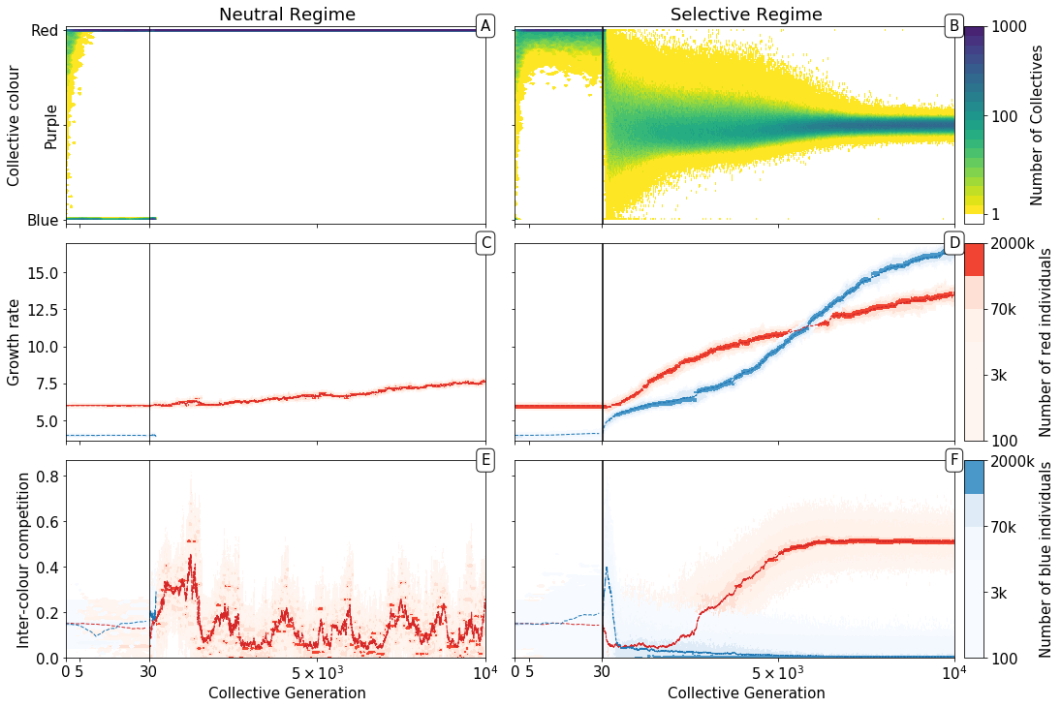

Figure 2: **Evolutionary dynamics of collectives and particles**. A population of D=1,000 collectives was allowed to evolve for $M = 10,000$ generations under the stochastic birth-death model described in the main text (see Appendix A for details on the algorithm used for the numerical simulations). Initially, each collective was composed of $B = 15$ particles of two types: red ($r = 6, a^{\text{intra}} = 0.8/K, a^{\text{inter}} = 0.15/K$) and blue ($r = 4, a^{\text{intra}} = 0.3, a^{\text{inter}} = 0.15$), with $K = 1,500$. The proportions at generation 0 were randomly drawn from a uniform distribution. At the beginning of every successive collective generation, each offspring collective was seeded with founding particles sampled from its parent. Particles were then grown for a duration of $T = 1$. When the adult stage was attained, 200 ($\rho = 20\%$) collectives were extinguished, allowing opportunity for extant collectives to reproduce. Collectives were marked for extinction either uniformly at random (*neutral regime*, panels *A,C,E*), or based on departure of the adult colour from the optimal purple colour ($\hat{\phi} = 0.5$) (*selective regime*, *B,D,F*). Panels A and B, respectively, show how the distribution of the red to blue ratio within collectives changes in the absence and presence of selection on collective colour. The first 30 collective generations (before the grey line) are magnified in order to make apparent early rapid changes. In the absence of collective-level selection purple collectives are lost in fewer than 10 generations leaving only red collectives (A) whereas purple collectives are maintained in the selective regime (B). Selection for purple-coloured collectives drives evolutionary increase in particle growth rate (D) compared to the neutral regime (C). In the neutral regime, inter-colour evolution of competition traits are driven by drift (E), whereas with collective level selection density-dependent interaction rates between particles of different colours rapidly achieve evolutionarily stable values (F).

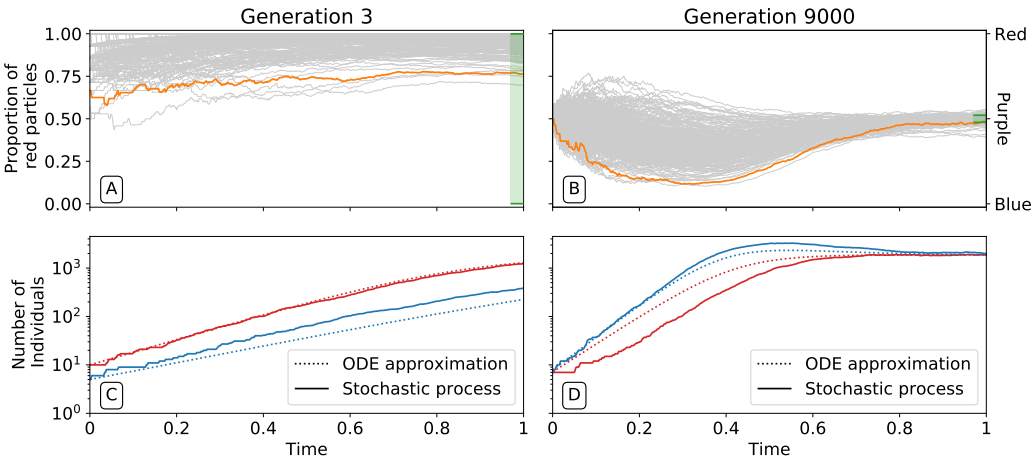

Figure 3: **Ecological dynamics of particles**. A sample of 300 (from a total of $1,000$) collectives were taken from each of generations 3 (A,C) and $9,000$ (B,D) in the evolutionary trajectory of Figure 2. The dynamic of particles was simulated through a single collective generation ($0 \leq t \leq T = 1$), based on the particle traits of each collective. Each grey line denotes a single collective. The green area indicates the $1 - \rho$=80% fraction of collectives in the whole population whose adult colour is closest to $\hat{\phi} = 0.5$. Single orange lines indicate collectives whose growth dynamic – number of individual particles – is shown in C and D, respectively. Dotted lines show the deterministic approximation of the particle numbers during growth (Appendix B Equation 1). Initial trait values result in exponential growth of particles (C), leading to a systematic bias in collective colour toward fast growing types (A). Derived trait values after selection yield a saturating growth toward an equilibrium (B) leading to the re-establishment of the purple colour by the end of the generation, despite initial departure (A).

part of the growth phase (Figure 3D). Compensation is a consequence of the evolution of inter-colour competition traits (Figure 2F). Population expansion is in turn dependent upon earlier increases in particle growth rate (Figure 2D).

The ability of offspring collectives to correct departures from the optimal colour during the course of growth is akin to a developmental, or canalising process: irrespective of phenotype of the newborn (which will invariably be different to that of the adult) the child – as it grows to adulthood – develops a phenotype that closely resembles that of the parent. Evidence of this apparent canalising process can be seen upon removal of collective-level selection (Figure 4). Collectives founded by particles with ancestral traits become composed of a single (red or blue) colour in less than 10 generations (Figure 4A). In contrast, derived collectives are comprised of particles whose traits ensure that collectives continue to give rise to offspring collectives expressing the optimal (purple) phenotype (as long as mutation is turned off (Figure 4B)). Even when mutation is allowed to drive within and between collective dynamics, stability of phenoytpe holds for more than 200 generations (Appendix A Figure 4).

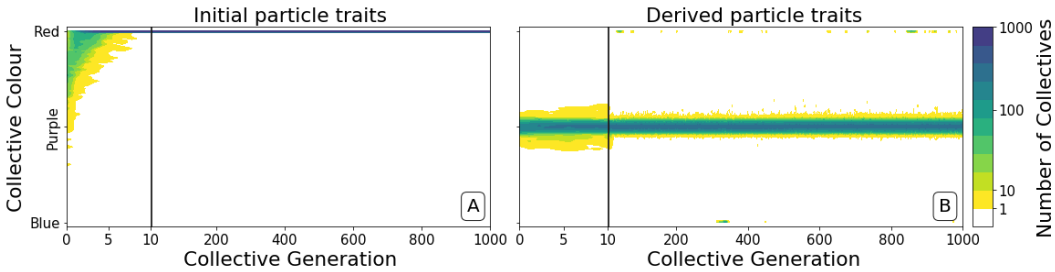

Figure 4: **Dynamics of ancestral and derived collectives in the neutral regime**. Comparison of the dynamics of the colour distribution after removing selection (neutral regime). The population of $1,000$ collective is initially composed of collectives with a colour distribution identical to that at generation $10,000$ in Figure 2B. Particle traits are: (A) as in generation 1 of Figure 2; (B) derived after 10,000 generations of collective level selection for purple. In both instances particle mutation was turned off in order to focus on ecological dynamics, otherwise parameters are the same as in Figure 2 A. Appendix A Figure 4 shows the outcome with particle mutation turned on. The first 10 collective generations are magnified in order to make apparent the initial rapid changes. The particle traits derived after evolution are such that the majority of collectives maintains a composition close to the optimum $\hat{\phi}$ even when the selective pressure is removed. This feature is instead rapidly lost in populations of collectives with the same initial colour, but with particle traits not tuned by evolution.

1.3 From particle ecology to collective phenotype

To understand the mechanistic basis of the canalising process it is necessary to understand the link between particle traits and the evolutionary emergence of the capacity of collectives to re-establish the parental-collective colour. Figure 5 shows the relationship between the initial colour of collectives at the moment of birth (the moment immediately following dilution ($t = 0$, newborn colour) and collective colour after a single particle growth cycle (the moment immediately preceding dilution ($t = T$, adult colour). Panel 5A shows this

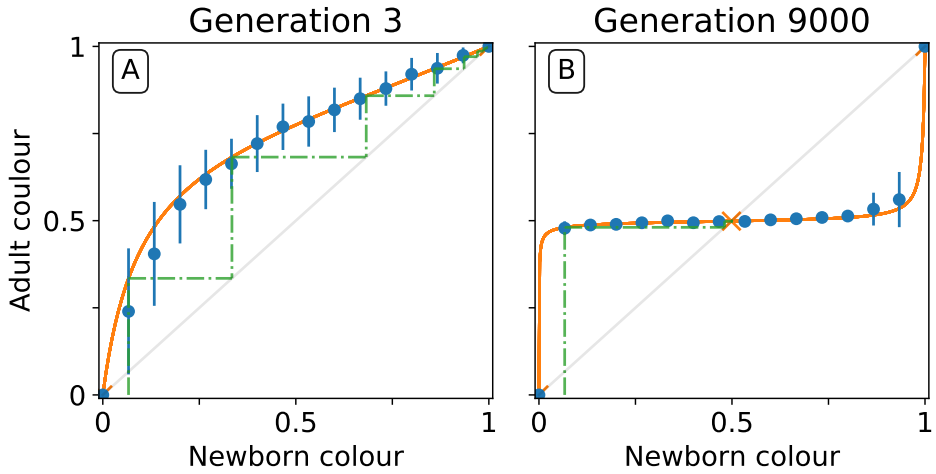

Figure 5: **Effect of collective level selection on newborn to adult dynamics**. The adult colour of collectives as a function of their newborn colour is displayed for collectives of uniformly distributed initial colour. Stochastic simulations are realized by using particle traits representative of: A) generation 3 (Figures 3C) and B) generation 9000 (Figure 3D). Blue dots indicate the mean adult colour from 50 simulations and its standard deviation. The orange line depicts the growth function G for the corresponding deterministic approximation (see main text and Appendix B). The green dashed line traces the discrete-time deterministic dynamics of the collective colour, starting from $\phi = 0.8$, and across cycles of growth and noise-less dilution. For ancestral particle traits, collective colour converges towards the red monochromatic fixed point (A). Selection for collective colour produces a growth function such that the optimum colour $\hat{\phi}$) is reliably produced within a single generation for almost all the range of possible founding colour ratio (B). The latter mechanism ensures efficient correction of alea occurring at birth and during development.

relationship at generation 3 while Panel 5B shows this relationship at generation $9,000$ of the selective regime.

At generation 3, the proportion of red particles increases irrespective of the initial proportion. This is because red particles grow faster than blue and the primary determinant of particle success is growth rate (particles spend no time in stationary phase). Thus, the only way that purple collectives can be maintained is if growth or reproduction are sufficiently noisy to ensure that some collectives happen by chance to be purple, due to, for example, stochastic effects associated with dilution. Accordingly, there is no mechanism that ensures that offspring collectives resemble parental collectives. The only way for purple-coloured collectives to be maintained is via strong purifying selection that would act to purge collectives that are either too red or too blue. A phenomenon referred to as stochastic correction (Maynard Smith and Szathmary, 1995; Grey et al., 1995; Johnston and Jones, 2015).

This is in marked contrast to the situation at generation $9,000$ where the proportion of red particles increases when the initial proportion is below 0.5 (the optimal proportion that defines the colour purple) and decreases when the initial proportion is above 0.5. Thus at generation $9,000$, irrespective of initial conditions, the final colour of any given collective after a single growth cycle will be closer to $\hat{\phi} = 0.5$ than it was on founding. Accordingly, extreme purifying selection is no longer required to maintain the parent-offspring relationship. Indeed, offspring collectives return to the parent phenotype even when the phenotype (at birth) departs significantly from the parent (adult) phenotype due to, for example, stochastic effects arising at the time of dilution. This "correction" stems from the ecological dynamics of the particles and resembles a developmental process. Hereafter we refer to this correction process as the *developmental corrector*.

The relationship between "newborn" and "adult" colour of collectives shown in Figure 5 can be used to follow the fate of collectives over several cycles of growth and reproduction, provided the stochastic effects associated with the dilution phase are momentarily ignored. The iteration using particle trait values from generation 3 is shown by the dotted line in Figure 5A (the adult colour of a collective is used as the newborn colour for the next cycle following a "staircase" geometric procedure). Because red particles grow faster than blue, it takes just six collective generations for red particles to fix within collectives. Conversely, after particle trait evolution (Figure 5B), the same staircase approach applied to newborn collectives of any colour shows rapid convergence to the colour purple (0.5) irrespective of the starting point. The difference in the relationship between initial and final colour at generation 3 and $9,000$ is evidence of the emergence of a mechanism for developmental correction.

In order to systematically explore the possible newborn-to-adult colour map and to understand how it changes through the evolution of particle traits, we use a deterministic approximation (orange line in Figure 5). This approximation is denoted G or *growth function* (Appendix B Definition B.1) and stems from an ordinary differential equation model often referred to as the competitive Lotka-Volterra system (Appendix B Equation 1). This model is the limit for vanishing noise of the stochastic particle ecology, and provides a good approximation of the simulations (Dotted lines in Figure 3C-D). The growth function G captures the outcome of the ecological dynamic after founding populations are allowed to grow for a finite time interval. We note similarity between the G function and the recently proposed "community-function landscape" (Xie and Shou, 2018). As such, it depends on the value of particle traits (growth rates $\mathbf{r} = [r_0, r_1]$, and competition parameters $\mathbf{A} = \{a_{ij}\}_{i,j\in\{0,1\}^2}$), but also on the bottleneck size at dilution B and the collective generation duration T. The fixed points of G (i.e., ϕ such as $G(\phi) = \phi$) are of particular interest: they represent colours

that are left unchanged during a generation according to the deterministic model. Fixed points are stable if the colour of collectives in their neighbourhood converges toward them (1 in Figure 5A, 0.5 in Figure 5B) or unstable otherwise (0 in Figure 5A, 0 and 1 in Figure 5B).

Under collective-level selection for colour, T and B are constant and particle traits evolve so that G eventually has a stable fixed point, corresponding to the target colour $\hat{\phi}$. Progressive change in the shape of the G function are illustrated in Figure 6 in a collective lineage from Figure 2B, across collective generations. Note that these changes are continuous: small mutations in particle traits reflect as small changes in the shape of G.

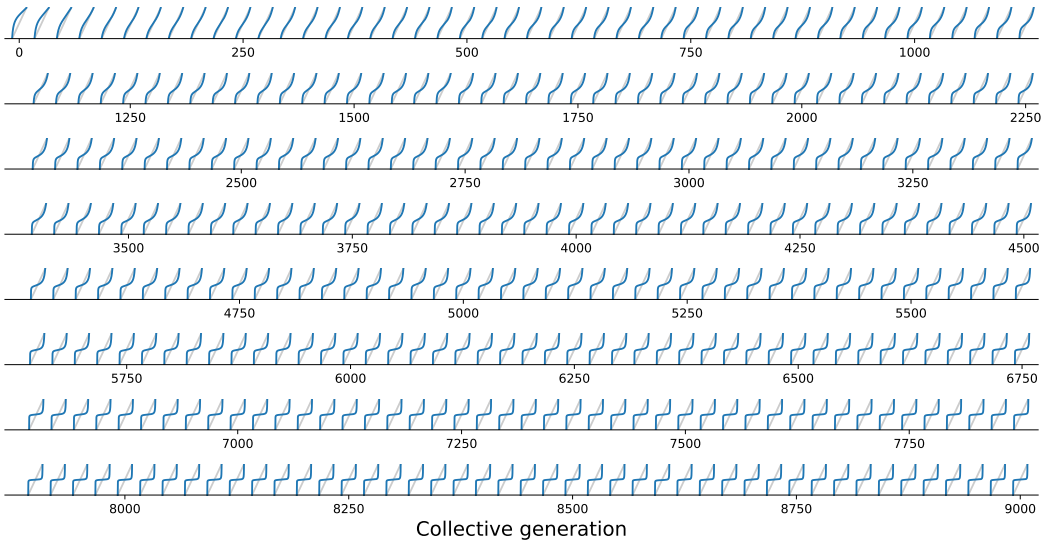

Figure 6: **Evolutionary variation of the growth function under collective selection**. G function associated with the resident types for a single lineage of collectives from the simulation of Figure 2B, plotted every 20 collective generations from 0 to 9000. The result of iterations of G gradually changes from fixation of the fast growing particle (Figure 7-1) to convergence toward a stable colour (Figure 7-4).

The evolutionary trajectory of Figure 2B can now be understood in terms of the progressive evolution of particle traits (see Appendix B for a detailed description). At the beginning, particles compete mostly during exponential phase, so that adult colour is biased towards the fast-growing type. Initial improvement in transmission of colour from parent to offspring arises as exponential growth rates r_i of the particles align. Correspondingly, the G function approaches linearity. A successive increase in maximal growth rate separates particle and collective time scales, allowing particles to experience density-dependent interactions. Eventually, such interactions evolve towards a regime where the G function is nonlinear and fluctuations are readily compensated, thus developmental correction ensures a reliable colour inheritance.

The G function, which allows characterisation of particle ecology, can now be used as a guidance to optimize the "life cycle" of growth and dilution that acts as a scaffold to the evolutionary process. In a typical experiment of community-level evolution, collective generation duration T and bottleneck size B are fixed. Some choices of these collective-level parameters are however likely to lead to collective phenotypes that are so far from the

optimum that collective lineages go extinct under a given selection rule. For instance, if in the first generation competitive exclusion occurs rapidly, then distinguishing collectives based on collective colour may be impossible. Intuition suggests that the closer the fixed point of the G function is to the target colour, the easier it will be to apply selection, and the faster the evolutionary dynamics. It is thus possible to use the distance between the fixed point of G and the target composition $\hat{\phi}$ as a proxy for the probability that collective lineages may go extinct before attaining the desired colour. Below, we examine how the position of the fixed point of G changes as a function of collective generation duration T and bottleneck size B.

1.4 Effect of collective generation duration and bottleneck size

The growth function G is readily computed from the particle traits and collective parameters even though it has in general no analytic expression (but see Appendix B for limit cases of exponential and saturating particle growth). There are four possible qualitative shapes of G, that differ in the position and stability of the fixed points (illustrated in Appendix B Figure 4-1 to 4-4).

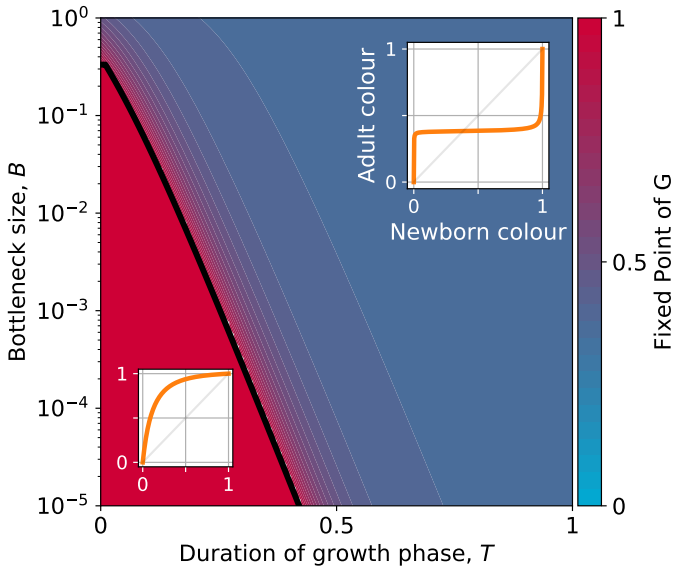

Figure 7: **Fixed point of G as a function of collective-level parameters**. Classification of the qualitative shape of the growth function and dependence on collective parameters B (bottleneck size) and T (growth phase duration), for the case when particle traits allow coexistence ($a_{01} < a_{11}$ and $a_{10} < a_{00}$, $r_0 > r_1$, see Appendix B Figure 4 for the other possible cases). The black line represents the limit of the region of stability of the fixed point of G, separating the two qualitatively different scenarios illustrated in the inset (see Appendix B Proposition 4): for short collective generations and small bottleneck size, the faster growing red type competitively excludes the blue type over multiple collective generations. In order for particles types to coexist over the long term, growth rate and the initial number of particles must both be large enough for density-dependent effects to manifest at the time when selection is applied.

The qualitative dependence of G and its fixed points on collective-level parameters varies with the underpinning particle ecology, making it easier for some communities to be starting points for the successful evolution of inheritance. Particle traits can be classified in four broad classes, based of the nature of the corresponding ecological equilibrium. For each of theses classes, and when red particles grow faster than blue $r_0 > r_1$, the fixed points of G are illustrated in Figure 4-A to 4-D) of Appendix B as a function of the collective-level parameters B and T. Figure 7 refers to the relevant class where inter-colour interaction traits are smaller than the intra-colour interaction traits. Here, the particle populations converge in the long term to a coexistence equilibrium, where collective colour is $\phi^* = \frac{a_{11}-a_{01}}{a_{11}-a_{01}+a_{00}-a_{10}}$ (in general, different from the optimum). This equilibrium can be approached within a single collective generation if T and B are large (top right corner). On the other hand, when T and B are small (red region), the only stable fixed point corresponds to a collective composed solely of fast-growing particles. This corresponds to cases where individual and collective time scales (quantified by r^{-1} and T) are insufficiently separated, or newborn size is too small, so that particle demography is essentially exponential and interactions cannot provide sufficient correction. In order to speed up evolution of purple colour, thus, the best is for collective generation duration and bottleneck size to have intermediate values. Knowledge of the exact values requires however some preliminary measure of the ecological dynamics. Even in the absence of such information, the diagram in Figure 7 can be used to orient experimental design by revealing intrinsic trade-offs. A decrease in generation time, necessary for practical reasons, may for instance be compensated by an increase in bottleneck size, without affecting the average collective phenotype.

Even when collective-level parameters are optimized so that the attractor of the G function is initially close to the target colour, collective-level selection will keep acting on the particle traits, and affect phenotypic variability within the population of collectives. As stability of the fixed point increases, so does fidelity of phenotype transmission from parent to offspring collectives. Once collective-level processes are set as to minimize the probability of collective extinction, the main obstacles to evolving higher inheritance come from constrains acting on particle traits, that may limit the range of attainable G functions. Trade-offs on particle ecology indeed may prevent the G function to attain an internal fixed point. We will discuss two examples on constrained evolution in the following paragraph.

1.5 Constrained trajectories

Thus far we have considered evolution within a four-dimensional parameter space defined by maximum growth rates and inter-color competition parameters. In real systems, however, constrains and trade-offs may limit the range of achievable variations in particle traits. For instance, even though faster-growing particles will always experience positive selection, cell replication rate cannot increase boundlessly. Here we consider two instances of constrained evolution, where only a subset of particle traits are allowed to mutate.

First, we consider the case where competition parameters are vanishingly small, so that G has no internal fixed point. Under such conditions, particle growth rates evolve to be identical (Figure 8A). In the absence of interactions, this is the only available solution to maintain collectives with an equal number of red and blue types. Under these circumstances, G is the identity function. In the deterministic approximation, collective composition remains constant in time, but stochastic fluctuations that cause colour to deviate from the optimum will be amplified across collective generations. These deviations are nonetheless corrected in the collective population by propagating only those collectives whose colour is

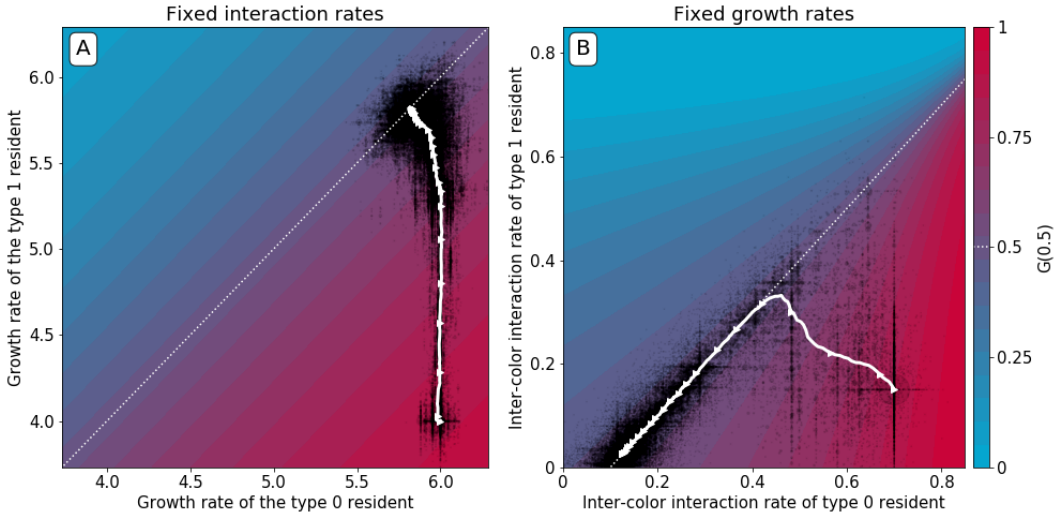

Figure 8: **Constrained evolutionary trajectories.** Changes in time of resident particle traits (black dots, whose size measures their abundance in the collective population) along simulated evolutionary trajectories of 300 generations, when particle-level parameters are constrained. For both panels $D = 1000, \hat{\phi} = 0.5, \rho = 20\%$, B=15, and $T = 1$. The trajectory of the average resident traits is shown in white. The heatmap represents the value of $G(0.5)$ as a function of the evolvable traits, and the white dotted line indicates where collective colour is optimum. A) Particle growth rates evolve and particles do not compete ($a_{\text{inter}} = a_{intra} = 0$). The evolutionary dynamics leads to alignment of growth rates ($r_0 = r_1$). B) Inter-colour competition traits evolve and particle growth rates are constant ($r_0 = r_1 = 25$). The evolutionary dynamics first converges toward the optimality line. In a second time, asymmetric competition evolves: $a_1^{\text{inter}} \lim 0$ and $a_0^{\text{inter}} \lim a_0^{\text{intra}} - a_1^{\text{intra}}$. This results in a flatter G function around the fixed point, providing a faster convergence to optimum colour across collective generations (Appendix B Figure 6). Similar results are obtained for non-identical, but sufficiently high, growth rates.

closest to the optimum. Such stochastic correction (Maynard Smith and Szathmary, 1995), however, has a high risk of failure if selection is strong and collective population size small.

Optimisation of the developmental corrector mechanism can instead occur when mutations only affect the two inter-type competition parameters, while growth rates are held constant (to sufficiently high values, so that particles experience density-dependent effects in the growth phase). The evolutionary trajectory can be visualized in the plane of the interaction parameters (a_{01}, a_{10}). Figure 8B shows the result of a stochastic simulation superimposed to the value of $G(0.5)$. Independent of the initial values of the interaction parameters, evolution draws the system to the manifold associated with the optimal proportion $\hat{\phi}$ (white dashed line). This is neutral in the deterministic approximation, but the presence of stochastic fluctuations drives further improvement of the fitness landscape. Correction is indeed more efficient and the distribution of collective phenotypic diversity narrower when the gradient of G in the fixed point is smaller. The condition on particle traits for the latter to vanish only depends on the carrying capacities of the two particle types, and corresponds to the type with smallest carrying capacity having a null interaction rate (see Appendix B). Developmental correction thus selects for maximal asymmetry in interactions, whereby one particle type drives the ecological dynamics of the other type, but is itself only affected by its own type .

2 Discussion

In nature, communities rarely ever qualify as units of selection in the traditional sense (Lewontin, 1970; Godfrey-Smith, 2009), because communities in nature rarely manifest heritable variance in fitness. In the laboratory however, experimenters can exogenously impose (scaffold) Darwinian-like properties on communities such that they have no choice, but to become units of selection (Wilson and Sober, 1989; Xie et al., 2019; Black et al., 2019). This typically involves placement of communities in some kind of container (pot, test-tube, flask, droplet, etc.) so they are bounded and variation at the community level is thus discrete. Communities are then allowed time for individual members to replicate and interact. At the end of the "growth" period, community function is assessed based on pre-determined criteria. The experimenter then effects replication of successful communities while discarding those that under-perform. Replication typically involves transferring a sample of individuals from a successful community to a new container replete with a fresh supply of nutrients.

Experimental and theoretical studies demonstrate that artificial selection on microbial communities results in rapid functional improvement (Swenson et al., 2000a,b; Goodnight, 2000; Wade, 2016; Xie et al., 2019). This is not unexpected given that experimental manipulations ensure that communities engage directly in the process of evolution by (artificial) selection in their own right. Nonetheless, there is understandable scepticism which stems for lack of understanding of the mechanistic basis of community-level heritability.

From the perspective of the Lewontin conditions, manipulations to communities such as those described above ensure that there exists variation among communities (assured by placing bounds around communities). Similarly, differential reproduction is evident by the fact that successful communities avoid extinction and typically leave multiple descendent communities. Heritability is less clear cut. Provided mixing of communities is avoided at the time of propagation, then offspring communities will be comprised of individuals that are themselves descendants of parental communities. But given stochastic effects associated with sampling and ensuing replication of individual members, this alone will not ensure that

the phenotype of offspring communities resembles that of the parental types.

Consideration of both the effectiveness of artificial selection and the problem of heredity led to early recognition that the answer likely lies in interactions (Wilson and Sober, 1989; Swenson et al., 2000a,b; Goodnight, 2000; Rainey et al., 2017). The intuition stems from the fact that in the absence of interactions, communities selected to reproduce because of their beneficial phenotype, will likely fail to produce offspring communities with the same (or better) functionality. If so, then these communities will be eliminated at the next round. Consider however, an optimal community in which interactions emerge among individuals that increase the chance that offspring communities resemble the parental type. Such an offspring community will then likely avoid extinction at the next round: selection at the level of communities is thus expected to favour the evolution of interactions because heritability of phenotype is now the primary determinant of the success of communities (at the community level). Indeed, simulations of multi-species assemblages have shown that evolution of interaction rates not only improves diversity-dependent fitness, but also increases collective "heritability", defined as the capacity of randomly seeded offspring communities to reach the same dynamical state as their parents (Ikegami and Hashimoto, 2002; Penn, 2003). Further studies have stressed the role of the extracellular environment and of specific interaction networks, pointing out that microscopic constrains can affect the capacity of communities to participate in evolutionary dynamics at the the higher level (Williams and Lenton, 2007; Xie and Shou, 2018; Xie et al., 2019).

Here, inspired by advances in millifluidics, we have developed a minimal mechanistic model containing essential ingredients of multi-scale evolution and within-community competition. We considered collectives composed of two types of particles (red and blue) that interact by density-dependent competition. By explicitly modelling demographic processes at two levels of organization, we have obtained mechanistic understanding of how selection on collective character affects evolution of composing particle traits. Between-collective selection fuels changes in particle-level traits that feed back to affect collective phenotype. Selection at the level of communities thus drives the evolution interactions among particles to the point where derived communities, despite stochastic effects associated with sampling at the moment of birth, give rise to offspring communities that reliably recapitulate the parental community phenotype. Such is the basis of community-level heredity. Significantly, it has arisen from the simplest of ingredients and marks an important initial step in the endogenisation of Darwinian properties: properties externally imposed stand to become endogenous (Black et al., 2019).

The mechanism by which particles interact to establish community phenoytpe is reminiscent of a development process. We refer to it as the "developmental corrector" mechanism. In essence, it is akin to canalisation, a central feature of development in complex living systems (Buss, 1987), and the basis of inheritance (Griesemer, 2002). Developmental correction solves the problem of implementing specific protocols for mitigating non-heritable variations in community function (Xie et al., 2019).

The developmental correction can be viewed as an evolutionary refinement of the stochastic corrector mechanism (Maynard Smith and Szathmary, 1995; Grey et al., 1995; Johnston and Jones, 2015). Both the stochastic and developmental correctors solve the problem of producing enough well-formed collectives at each successive generation to prevent community-level extinction. The stochastic corrector mechanism relies on a low-fidelity reproduction process coupled to high population sizes. Deviations from successful collective states are corrected by purging collectives that depart significantly from the optimal collective phenotype. However, in the absence of strong collective-level selection the optimal community phenotype

is rapidly lost. In contrast, the developmental corrector mechanism ensures that the optimal community phenotype is maintained without need for hard selection. Regardless of perturbations introduced by demography or low initial particle number, most collectives reliably reach a successful adult state. In our simulations, we show that community phenotype is maintained even in the absence of community-level selection, although ultimately mutational processes affecting particle dynamics result in eventual loss of the corrector mechanism.

An operationally relevant question concerns the conditions (the initial state of the population, the nature of the scaffold and of particle-level interactions) for selection on a collective character to result in evolution of developmental correction. While we did not detail the probability of collective lineage extinction, it is possible that collectives become monochromatic before evolution has had time to act on particle traits. In such cases, which are more likely if particle-level parameters are far from the Lotka-Volterra coexistence equilibrium (Figure 7), and if time-scales of particle and collective generations are not well separated, then collective-level evolution will grind to a halt. In all other cases, provided there are no other evolutionary constraints, selection will eventually lead the system toward regions of particle parameter space where the collective phenotype becomes reliably re-established. The efficiency of this selective process and its transient behaviour depends on collective-level parameters that control growth and reproduction.

From our models and simulations it is clear that once density-dependent interactions govern the adult state then collective-level selection for colour is promptly effected. This happens provided the intra-collective ecology lasts long enough for nonlinear effects to curb particle growth. When this is not the case, for example when the bottleneck at birth is small, or collective-level generation time is short, evolution of developmental correction will be impeded. The latter favours rapidly growing particles and offers little possibility for the evolution of developmental correction (Abreu et al., 2019). When the ecological attractor within collectives leads to the extinction of one of the two types, long collective-level generation times are incompatible with the maintenance of both types (van Vliet and Doebeli, 2019). However, in our model, particle-level evolution changes the nature of the attractor from extinction of one of the two types to stable coexistence and particle and collective time-scales become separate. Even before developmental correction becomes established, evolution can transiently rely on stochastic correction to ensure the maintenance of particle co-existence.

There are two aspects to heredity: resemblance — the extent to which reproduction and development systematically bias offspring phenotypes — and fidelity (or determination) — a measure of the variance among offspring phenotypes (Jacquard, 1983; Bourrat, 2017). In our model, resemblance arises from the moment that density-dependent interactions counter the bias toward fast replicating particles: once the G function has an internal fixed point in $\hat{\phi}$, systematic drift of collective colour is prevented. As a consequence, the collective phenotype is placed under the control of particle traits rather than demographic stochasticity. Fidelity improves after resemblance has been achieved and is associated with progressive divergence of particle and collective demographic time scales.

The fine-tuning of collective-level heritability occurs by changes in interaction parameters under the constraint that they do not affect average adult colour. Instead, the variance of cross-generational phenotype variation is reduced by increasing canalization (flattening of the G function). This is best achieved by a strong asymmetry in the competition traits, whereby one type has a logistic, uncoupled, dynamic, and the second type adjusts its growth to the former's density. In the Lotka-Volterra competition model used here, it is always the type with the lower carrying capacity, regardless of its relative growth rate, that acts as

the driver. The extent to which this conclusion is generally applicable to the evolution of synthetic communities will require future exploration of a broader range of particle-level ecologies. Possibilities to make community dynamics more realistic by complexifying mathematical descriptions of particle-level processes are plentiful (Williams and Lenton, 2007; Zomorrodi and Segrè, 2016). Of particular interest for the evolution of efficient developmental correction are cases when community ecology has multiple attractors (Penn and Harvey, 2004), is highly sensitive to initial conditions (Swenson et al., 2000b), or presents finite-effect mutations sustaining "eco-evolutionary tunnelling" (Kotil and Vetsigian, 2018).

The simple density-dependent developmental corrector we have elucidated here captures early events that may have underpinned egalitarian transitions in individuality involving integration of independently reproducing units (Queller, 1997). It is not inconceivable that a biological analog of the red-blue particle model performed with red and blue coloured bacteria – where there exist many possibilities for interactions to evolve beyond simple density dependence – might eventually result in communities in which the replicative fates of individuals become aligned to the point where they are no longer divisible. For example, during evolution of the eukaryotic cell one cell type invaded (or was engulfed) by a second (Martin and Müller, 1998). Further extension of our model is readily possible because of abstract nature of particles that might represent a diversity of entities underpinning, for example, emergence of the protocell (Takeuchi and Hogeweg, 2009; Baum and Vetsigian, 2017), evolution of chromosomes from genes, or evolution of the eukaryotic cell from separate bacteria. In all these cases, maintenance of particle types in optimal proportions was an essential step. Density-dependant correction is found in bacterial plasmids (Eberhard, 1990) and their chromosomes-like counterpart chromids (Harrison et al., 2010) but it is not the mechanism observed in organelle number control (Cole, 2016; Jajoo et al., 2016) or chromosome segregation (Badrinarayanan et al., 2015). However, it provides a simple initial mechanism that can act as a "ratchet" (Libby and Ratcliff, 2014), paving the way to further enhancement of collective phenotype inheritance.

3 Acknowledgments

GD is funded by the *Origines et Conditions d'Apparition de la Vie (OCAV)* programme, PSL University (ANR-10-IDEX-001-02), SDM was supported by the French Government under the program Investissements d'Avenir (ANR-10-LABX-54 MEMOLIFE and ANR-11-IDEX-0001-02PSL).

References

Abreu, C. I., Friedman, J., Woltz, V. L. A., and Gore, J. (2019). Mortality causes universal changes in microbial community composition. *Nature Communications*, 10(1):1–9.

Badrinarayanan, A., Le, T. B., and Laub, M. T. (2015). Bacterial Chromosome Organization and Segregation. *Annual Review of Cell and Developmental Biology*, 31(1):171–199.

Baum, D. A. and Vetsigian, K. (2017). An Experimental Framework for Generating Evolvable Chemical Systems in the Laboratory. *Origins of Life and Evolution of Biospheres*, 47(4):481–497.

Black, A. J., Bourrat, P., and Rainey, P. B. (2019). Ecological scaffolding and the evolution of individuality: the transition from cells to multicellular life. *bioRxiv*, page 656660.

Bonner, J. T. (1982). Evolutionary strategies and developmental constraints in the cellular slime molds. *The American Naturalist*, 119(4):530–552.

Bourrat, P. (2017). Evolutionary Transitions in Heritability and Individuality. *bioRxiv*, page 192443.

Buss, L. W. (1982). Somatic cell parasitism and the evolution of somatic tissue compatibility. *Proceedings of the National Academy of Sciences*, 79(17):5337–5341.

Buss, L. W. (1987). *The evolution of individuality*. Princeton University Press, Princeton.

Champagnat, N., Ferrière, R., and Méléard, S. (2006). Unifying evolutionary dynamics: From individual stochastic processes to macroscopic models. *Theoretical Population Biology*, 69(3):297–321.

Cole, L. W. (2016). The Evolution of Per-cell Organelle Number. *Frontiers in Cell and Developmental Biology*, 4.

Day, M. D., Beck, D., and Foster, J. A. (2011). Microbial Communities as Experimental Units. *BioScience*, 61(5):398–406.

De Monte, S. and Rainey, P. B. (2014). Nascent multicellular life and the emergence of individuality. *Journal of Biosciences*, 39(2):237–248.

Doebeli, M., Ispolatov, Y., and Simon, B. (2017). Point of View: Towards a mechanistic foundation of evolutionary theory. *eLife*, 6:e23804.

Eberhard, W. G. (1990). Evolution in Bacterial Plasmids and Levels of Selection. *The Quarterly Review of Biology*, 65(1):3–22.

Geritz, S. A. H., Kisdi, E., Meszéna, G., and Metz, J. a. J. (1998). Evolutionarily singular strategies and the adaptive growth and branching of the evolutionary tree. *Evolutionary Ecology*, 12(1):35–57.

Gillespie, D. T. (2001). Approximate accelerated stochastic simulation of chemically reacting systems. *The Journal of Chemical Physics*, 115(4):1716–1733.

Godfrey-Smith, P. (2009). *Darwinian Populations and Natural Selection*. Oxford university Press, Oxford.

Goodnight, C. and Stevens, L. (1997). Experimental Studies of Group Selection: What Do They Tell Us about Group Selection in Nature? *The American Naturalist*, 150(S1):S59–S79.

Goodnight, C. J. (2000). Heritability at the ecosystem level. *Proceedings of the National Academy of Sciences*, 97(17):9365–9366.

Grey, D., Hutson, V., and Szathmáry, E. (1995). A re-exam ination of the stochastic corrector model. *Proc. R. Soc. Lond. B*, 262(1363):29–35.

Griesemer, J. (2002). What is "epi" about epigenetics? *Annals of the New York Academy of Sciences*, 981(1):97–110.

Hammerschmidt, K., Rose, C. J., Kerr, B., and Rainey, P. B. (2014). Life cycles, fitness decoupling and the evolution of multicellularity. *Nature*, 515(7525):75–79.

Harrison, P. W., Lower, R. P. J., Kim, N. K. D., and Young, J. P. W. (2010). Introducing the bacterial 'chromid': not a chromosome, not a plasmid. *Trends in Microbiology*, 18(4):141–148.

Ikegami, T. and Hashimoto, K. (2002). Dynamical Systems Approach to Higher-level Heritability. *Journal of Biological Physics*, 28(4):799–804.

Jacquard, A. (1983). Heritability: One Word, Three Concepts. *Biometrics*, 39(2):465–477.

Jajoo, R., Jung, Y., Huh, D., Viana, M. P., Rafelski, S. M., Springer, M., and Paulsson, J. (2016). Accurate concentration control of mitochondria and nucleoids. *Science*, 351(6269):169–172.

Johnson, C. R. and Boerlijst, M. C. (2002). Selection at the level of the community: the importance of spatial structure. *Trends in Ecology & Evolution*, 17(2):83–90.

Johnston, I. G. and Jones, N. S. (2015). Closed-form stochastic solutions for non-equilibrium dynamics and inheritance of cellular components over many cell divisions. *Proc. R. Soc. A*, 471(2180):20150050.

Kotil, S. E. and Vetsigian, K. (2018). Emergence of evolutionarily stable communities through eco-evolutionary tunnelling. *Nature Ecology & Evolution*, 2(10):1644–1653.

Lewontin, R. C. (1970). The Units of Selection. *Annual Review of Ecology and Systematics*, 1:1–18.

Libby, E. and Ratcliff, W. C. (2014). Ratcheting the evolution of multicellularity. *Science*, 346(6208):426–427.

Margulis, L. (1970). *Origin of eukaryotic cells: evidence and research implications for a theory of the origin and evolution of microbial, plant, and animal cells on the precambrian earth.* Yale University Press, New Haven, USA.

Martin, W. and Müller, M. (1998). The hydrogen hypothesis for the first eukaryote. *Nature*, 392(6671):37–41.

Maynard Smith, J. and Szathmary, E. (1995). *The Major Transitions in Evolution.* W.H. Freeman, Oxford.

Penn, A. (2003). Modelling artificial ecosystem selection: A preliminary investigation. In *European Conference on Artificial Life*, pages 659–666. Springer.

Penn, A. and Harvey, I. (2004). The Role of Non-Genetic Change in the Heritability, Variation, and Response to Selection of Artificially Selected Ecosystems. In *Artificial Life IX: Proceedings of the Ninth International Conference on the Simulation and Synthesis of Artificial Life*, volume 9, page 352. MIT Press.

Queller, D. C. (1997). *Cooperators since life began.* University of Chicago Press.

Rainey, P. B., Remigi, P., Farr, A. D., and Lind, P. A. (2017). Darwin was right: where now for experimental evolution? *Current Opinion in Genetics & Development*, 47:102–109.

Sackmann, E. K., Fulton, A. L., and Beebe, D. J. (2014). The present and future role of microfluidics in biomedical research. *Nature*, 507(7491):181–189.

Swenson, W., Arendt, J., and Wilson, D. S. (2000a). Artificial selection of microbial ecosystems for 3-chloroaniline biodegradation. *Environmental Microbiology*, 2(5):564–571.

Swenson, W., Wilson, D. S., and Elias, R. (2000b). Artificial ecosystem selection. *Proceedings of the National Academy of Sciences*, 97(16):9110–9114.

Takeuchi, N. and Hogeweg, P. (2009). Multilevel Selection in Models of Prebiotic Evolution II: A Direct Comparison of Compartmentalization and Spatial Self-Organization. *PLOS Computational Biology*, 5(10):e1000542.

van Vliet, S. and Doebeli, M. (2019). The role of multilevel selection in host microbiome evolution. *Proceedings of the National Academy of Sciences*, 116(41):20591–20597.

Wade, M. J. (2016). *Adaptation in Metapopulations*.

Williams, H. T. P. and Lenton, T. M. (2007). Artificial selection of simulated microbial ecosystems. *Proceedings of the National Academy of Sciences*, 104(21):8918–8923.

Wilson, D. S. and Knollenberg, W. G. (1987). Adaptive indirect effects: the fitness of burying beetles with and without their phoretic mites. *Evolutionary Ecology*, 1(2):139–159.

Wilson, D. S. and Sober, E. (1989). Reviving the superorganism. *Journal of Theoretical Biology*, 136(3):337–356.

Wilson, E. O. (1985). The Sociogenesis of Insect Colonies. *Science*, 228(4707):1489–1495.

Xie, L. and Shou, W. (2018). Community function landscape and steady state species ratio shape the eco-evolutionary dynamics of artificial community selection. *bioRxiv*, page 264697.

Xie, L., Yuan, A. E., and Shou, W. (2019). Simulations reveal challenges to artificial community selection and possible strategies for success. *PLOS Biology*, 17(6):e3000295.

Zomorrodi, A. R. and Segrè, D. (2016). Synthetic Ecology of Microbes: Mathematical Models and Applications. *Journal of Molecular Biology*, 428(5, Part B):837–861.

Appendix A

A Stochastic Model

This appendix presents an outline for the approximated stochastic simulation of the nested population dynamics described in the main text. For simplicity, the outline is first given for system in which particle population is monomorphic without mutation. Particle mutations are discussed in a second time. The full implementation of the model will be made available with the manuscript as a Python package.

A.1 Parameters

First we define a series of parameters for the system:

// **Parameters**
$D \leftarrow 1000$ // *Number of collectives*
$M \leftarrow 10,000$ // *Number of collective generations*
$B \leftarrow 15$ // *Bottleneck size*
$T \leftarrow 1.0$ // *Duration of a collective generation*
regime $\leftarrow$ selective // *Selective or Neutral regime*
$\rho \leftarrow 0.2$ // *Percentage of extinguished collective*
$\phi^* \leftarrow 0.5$ // *Optimal collective colour (for selective regime)*

Collectives are comprised of two kinds of self-replicating particles (red and blue) that carry a different set of traits. In this outline they are represented as global variables. In the full simulation procedure those traits can mutate (see the mutation section below).

// **Particle traits**
// *Carried by blue particles*
r_0 // *Maximum growth rate*
a_0^{intra} // *Competition with blue particles*
a_0^{inter} // *Competition with red particles*
// *Carried by red particles*
r_1 // *Maximum growth rate*
a_1^{intra} // *Competition with red particles*
a_1^{inter} // *Competition with blue particles*

The state variables store the trajectory of the system.

// **State variables**
$\mathbf{N}_0$ // *matrix of size D,M, number of blue individuals in each collective at each generation*
$\mathbf{N}_1$ // *matrix of size D,M, number of red individuals in each collective at each generation*
$\mathbf{\Phi}$ // *matrix of size D,M, proportion of red individuals in each collective at each generation*

A.2 Initial conditions

Initial conditions consists in defining the number of red and blue particle in each collective at generation 0.

procedure INITIAL CONDITIONS
  $x_0 \leftarrow 0.5$ // *Initial red-blue ratio*
  for d from 1 to D **do**
    $\mathbf{N}_0[d, 0] \leftarrow \text{RandomBinomial}(B, x_0)$
    $\mathbf{N}_1[d, 0] \leftarrow B - N_0[d, 0]$

A.3 Outline of the main loop

The main loop of the algorithm applies the sequence growth-selection-reproduction for each generation.

procedure MAIN LOOP
  for m from 1 to M **do**
    // *Particle Growth*
    for d from 1 to D **do**
      $\mathbf{N}_0[d, m], \mathbf{N}_1[d, m] \leftarrow \textsc{Growth}(\mathbf{N}_0[d, m], \mathbf{N}_1[d, m], r_0, r_1, a_0^{\text{intra}} a_0^{\text{inter}}, a_1^{\text{intra}} a_1^{\text{inter}})$
      $\mathbf{\Phi}[d, m] \leftarrow \mathbf{N}_1[d, m]/(\mathbf{N}_0[d, m] + \mathbf{N}_1[d, m])$
    // *Collective-level selection*
    parents $\leftarrow \textsc{Select_Collectives}(\mathbf{\Phi}[d, m], \rho, \phi^*)$
    // *Collective-level reproduction*
    for d from 1 to D **do**
      $N_0[d, m+1] \leftarrow \text{RandomBinomial}(B, \mathbf{\Phi}[\text{parents}[d], m])$
      $N_1[d, m+1] \leftarrow B - \mathbf{N}_0[d, m+1]$

A.4 Particle-level ecology

The ecological dynamics of particles is expressed by a multi-type birth-death process with a linear birth rate and a linearly density-dependent death rate. Each type of particle i is characterised by four traits: colour (c_i, red or blue), maximum growth rate r_i, and two density-dependent interaction parameters. Particles of the same colour interact according to a_i^{intra} whereas particles of different colour interact according to a_i^{inter}. Interactions terms are in the order of 0.1 and scaled by a carrying capacity term K. The dynamic is modelled by a continuous time Markov jump process with rates:

Each particle of type i ...	With rate...
Reproduces (add an particle of type i)	r_i
Dies (remove a particle of type i)	$r_i \left(\sum_j \delta_{c_i = c_j} x_j a_j^{\text{intra}} K^{-1} + \sum_j \delta_{c_i \neq c_j} x_j a_j^{\text{inter}} K^{-1} \right)$

Where $\delta_{i=i} = 1$ if $i = j$ or 0 if $i \neq j$. Additionally $\delta_{i \neq i} = 1$ if $i \neq j$ or 0 if $i = j$.

The stochastic trajectory of the system is simulated using a Poissonian approximation close to τ-leap algorithms (Gillespie, 2001), dt is chosen to be small enough so negative population size do not occur.

function GROWTH($n_0, n_1, r_0, r_1, a_0^{\text{intra}} a_0^{\text{inter}}, a_1^{\text{intra}} a_1^{\text{inter}}$)
  // *Stochastic simulation of the population dynamics*
  while t¡T **do**
    birth0 $\leftarrow$ RandomPoisson($dt \times n_0 r_0$)
    birth1 $\leftarrow$ RandomPoisson($dt \times n_1 r_1$)
    death0 $\leftarrow$ RandomPoisson($dt \times n_0 r_0 (n_0 a_0^{\text{intra}} + n_1 a_1^{\text{inter}})$)
    death1 $\leftarrow$ RandomPoisson($dt \times n_1 r_1 (n_0 a_0^{\text{inter}} + n1 a_1^{\text{intra}})$)
    $n_1 \leftarrow n_1$ + birth1 - death1
    $n_0 \leftarrow n_0$ + birth0 - death0
    t $\leftarrow$ t + dt
  Return n_0, n_1

Early test using an exact stochastic simulation algorithm (Doob-Gillespie SSA) did not exhibit qualitative changes in the trajectory, but greatly increase the computation duration.

A.5 Collective-level selection

The collective level selection phase consists in associating every of the D new collectives from generation $m+1$ with a single parent at generation m. In the main text we contrast two regimes: (colour) neutral and (colour) selective. In both cases a fixed proportion ρ of the collective population at generation m is marked for extinction. In the neutral regime, they are selected uniformly at random (Appendix A Figure 1A), whereas in the selective regime they are those that rank the highest in their distance to the optimal color ϕ^* (Appendix A Figure 1B). Each surviving collective is produces offspring. Moreover, the remaining collectives from generation $m+1$ are generated by a parent chosen uniformly at random from the set of surviving collective.

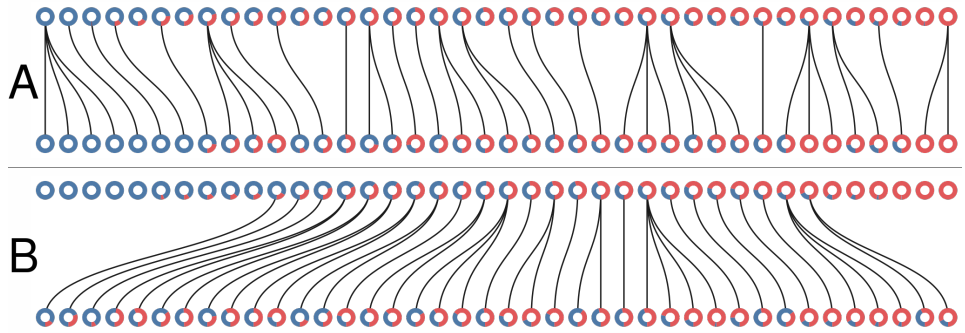

Figure 1: **Collective level selection regimes.** Each ring represents a collective. The blue section of the ring represents the proportion of blue particles at the adult stage of the collective. Parent and offspring are linked by a black line. A: One generation of the neutral regime. B: one generation of the selective regime. In both cases $M = 1,\ D = 40,\ \rho = 0.4$.

function SELECT_COLLECTIVES(ϕ, ρ, ϕ^*, regime)

```
// Return the indices of the new collectives' parents
surviving ← empty list          // indices of the surviving collectives
reproducing ← empty list          // indices of the reproducing collectives
parents ← empty list          // indices of the parent collectives
if regime is selective then
    threshold ← Percentile((φ − φ*)^2, ρ)
    for d from 1 to D do
        if (φ[d] − φ*)^2 < threshold then
            Add d to surviving
else if regime is neutral then
    surviving = RandomMultinomialWithoutReplacement(1...d, n = (1 − ρ)D)
// Extinct collectives are replaced by the offspring of a randomly drawn surviving collective
for 1 to D-Length(surviving) do
    Add RandomChoice(surviving) to reproducing
// Surviving collectives have at least one offspring, and the population size is kept constant by additional reproduction events.
parents ← Concatenate(surviving, reproducing)
Return parents
```

Other selection procedures can be implemented, such as randomly sampling ρD collective with weight based on the colour-deviation to the optimal colour. In our experience, the qualitative results of the model are robust to changes in the selective regime as long as collective with an optimal colour are favoured and the collective population does not go extinct.

Collective reproduction is implemented seeding an offspring collective with a sample of B particle drawn according to the proportion of the parent collective. We assume that the final particle population sizes are big enough so that each reproduction event can be modelled as an independent Binomial sample. Smaller population sizes might require simultaneous multinomial sampling of all offspring.

A.6 Mutation of particle traits

The complete model add the possibility for particle traits (r, a^{inter}) to mutate. Each collective contains two variants of each color. Whenever a variant goes extinct, the remaining type is called the 'resident', and a mutant type is created as follows. First, the traits of the resident are copied in one newborn particle, then one of the mutable traits, either the growth rate (r) or the inter-color competition trait (a_{inter}), is chosen at random, and finally a random value taken from a uniform distribution over $[-\varepsilon, \varepsilon]$ is added (in Figure 2, $\varepsilon = 0.1$). Traits are kept positive by taking the absolute value of the result. This process is in the spirit of adaptive dynamics in which invasion of new mutants is repeatedly assessed. We checked that relaxing this assumption (i.e. allowing more than two-types of each colour in each collective), or waiting that rare mutations appear did not change the qualitative results. The pseudo-code outlined above must be modified in order to track the trait value of both resident and mutant types in each collective, rather than having the traits values as global variables.

A.7 Supplementary Figures

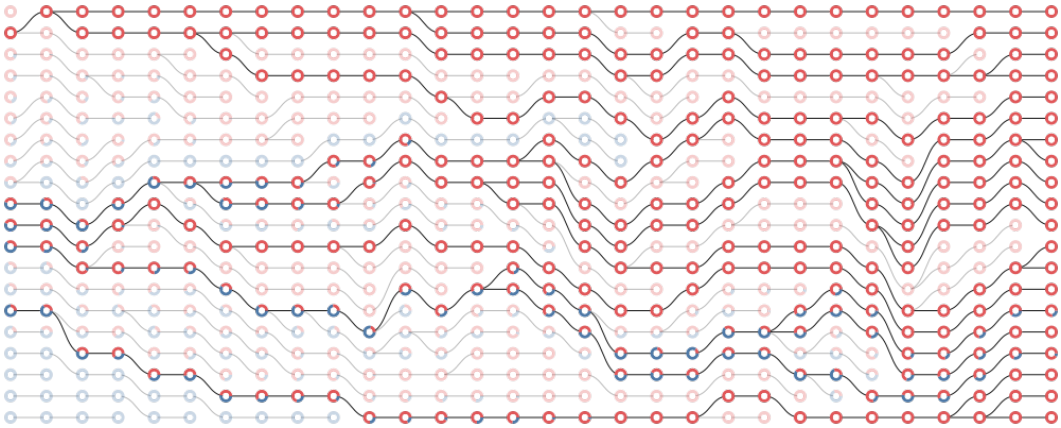

Figure 2: **An example of collective genealogy in the neutral regime.** The legend is identical than in Appendix A Figure 1. Extinct lineages are less opaque. $M = 30$, $D = 20$, $\rho = 0.1$. At the final generation, collectives are monochromatic, either all blue or all red.

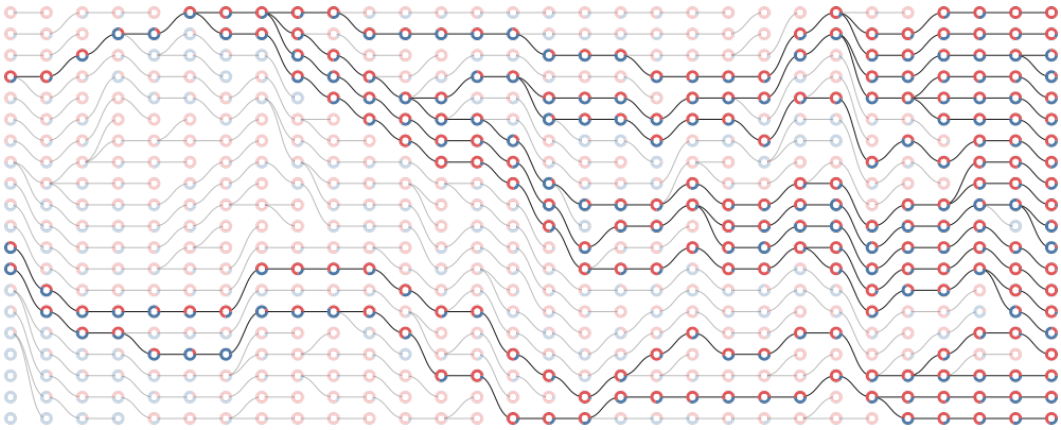

Figure 3: **An example of collective genealogy in the selective regime.** The legend is identical than in Appendix A Figure 1. Extinguished lineages are transparent. $M = 30$, $D = 20$, $\rho = 0.1$. At the final generation, collectives contain both red and blue particles.

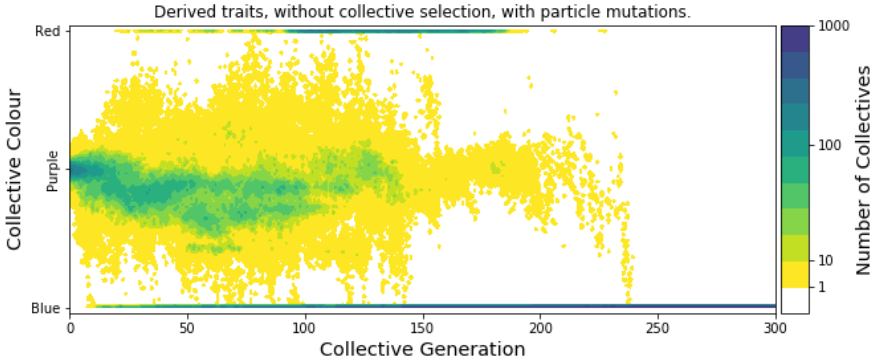

Figure 4: **Removing collective level selection, keeping mutations.** When collective-level selection is removed after $10,000$ generations (and mutation turned of, collectives continue to produce to purple offspring for more than 200 generations, before mutation erodes density-dependent self-correction. In contrast if the selective regime is not applied, red or blues particles are lost in less than 10 generations (Figure 2A).

Appendix B

B Lotka-Volterra deterministic particle ecology

B.1 Model for intra-collective dynamics

The stochastic ecological dynamics of red (N_0) and blue (N_1) particles within a collective simulated by the algorithm described in Appendix A is approximated (see Figure 3) by the deterministic competitive Lotka-Volterra Ordinary Differential Equation:

$$\begin{cases} \frac{dN_0}{dt} = r_0 N_0 \left(1 - \frac{a_{00}}{K} N_0 - \frac{a_{01}}{K} N_1\right) \\ \frac{dN_1}{dt} = r_1 N_1 \left(1 - \frac{a_{10}}{K} N_0 - \frac{a_{11}}{K} N_1\right) \end{cases} \tag{1}$$

Here, $r = [r_0, r_1]$ are the maximal growth rates of the red and blue particles. Since the system is symmetric, we will only consider the case when red particles grow faster than blue particles ($r_0 > r_1$). The effect of pairwise competitive interactions between cells are encoded in the matrix $A = (a_{ij})_{i,j \in \{0,1\}^2}$. All competitive interactions are considered harmful or neutral ($0 \leq a_{ij}$). No specific mechanism of interaction is assumed, so as to explore the space of all possible interaction intensities, and thus qualitatively different ecological dynamics of the particle populations.

The carrying capacity of a monochromatic collective is $\frac{K}{a_{00}}$ for red particles and $\frac{K}{a_{11}}$ for blue particles. K is a scaling factor for the intensity of pairwise iteration that can be used to rescale the deterministic system to match the stochastic trajectories. Without loss of generality, we thus assume that $K = 1$.

A natural set of alternate coordinates for the system in Equation 1 are total population size $N := N_0 + N_1$ and collective colour, defined as the frequency of red individuals $x := \frac{N_0}{N}$. In this coordinates the deterministic dynamics is the solution of the following ODE.

$$\begin{cases} \frac{dN}{dt} &= N g(x, N) \\ \frac{dx}{dt} &= x(1-x) h(x, N) \end{cases} \tag{2}$$

The applications g and h are polynomials in x and N, of coefficients:

Monomial	Coefficient in h	**Monomial**	Coefficient in g
1	$r_0 - r_1$	1	r_1
N	$a_{11} r_1 - a_{01} r_0$	N	$-a_{11} r_1$
Nx	$r_1(a_{10} - a_{11}) + r_0(a_{01} - a_{a00})$	x	$r_0 - r_1$
		xN	$r_1(2a_{11} - a_{10}) - r_0 a_{01}$
		$x^2 N$	$r_0(a_{01} - a_{00}) + r_1(a_{10} - a_{11})$

Figure 1 shows an example of the ODE flow in both coordinate systems. Here two unstable trivial equilibria and a stable coexistence equilibrium are located at the intersection of the isoclines. Within one collective generation, the dynamics will follow such flows for a duration T, starting from initial conditions on the line $N_0 = B - N_1$ ($N = B$).

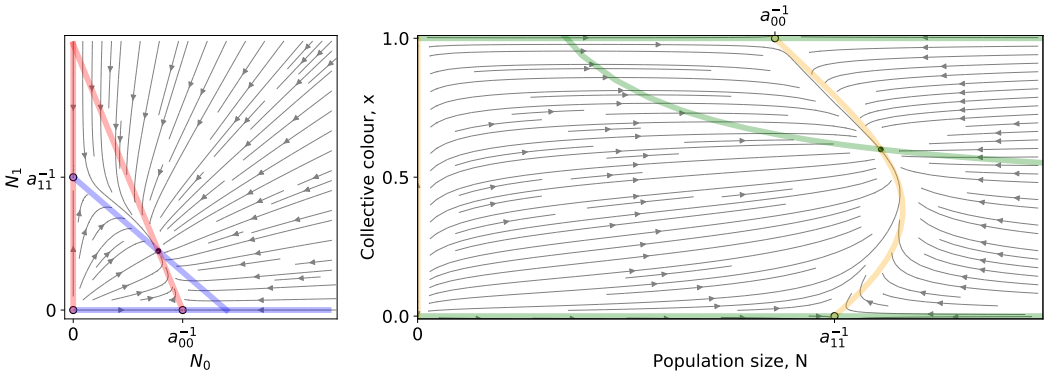

Figure 1: **Left:** A Lotka-Volterra flow (Eq 1) in (N_0, N_1) coordinates. **Right:** The same flow in (N, x) coordinates. Colored lines are the null isoclines. Empty (resp. filled) circles mark unstable (resp. stable) equilibria.

Even though Equation 1 is more directly related to the individual-based stochastic simulation, the dynamics of collective colour is understood more easily using Equation 2. Therefore, in the following we will use the latter formulation.

The dynamics of particle types across collective generations is modelled as a piecewise continuous time change, where $x^m(t)$ is the fraction of red particles at time $t \in [0, T]$ during collective generation m. We focus in particular on the succession $N^m(T), x^m(T)$ of collective "adult" state at the end of each successive generation. In the following we note $\phi^m = x^m(T)$ the adult colour of the collective at the end of the growth phase. At the beginning of each collective generation, we impose that every collective contains the same number of cells $\forall m, N^m(0) = B \in \mathbb{R}$. The newborn collective colour $x^m(0)$ will instead depend on the colour of the parent. For $m > 0$, we consider that there is no stochastic variation of the collective composition at birth, so that $x^m(0) = x^{m-1}(T) = \phi^{m-1}$. In the first generation ($m = 0$), the population size is B in every collective and the fraction of red particles is chosen uniformly at random between 0 and $K = 1$.

The proportion of red particles at adult stage ϕ^m is obtained from these initial conditions (B, ϕ^{m-1}) by integrating Equation 2. Since these equations are not explicitly solvable, there is no analytic expression for the result of the transient dynamics. However, having constrained the initial conditions to a single dimension, the adult colour is a single-valued function of the initial composition of the collective, defined as follows.

Definition (Growth function)**.** Given the set of particle traits $\theta := (r, A) \in E := \mathbb{R}_+^2 \times \mathbb{R}_+^4$, the bottleneck size $B \in \mathbb{R}_+^*$ and the duration of the growth phase $T \in \mathbb{R}_+^*$, the growth function G_θ is defined as the application that maps an initial proportion of red particles ϕ to the proportion of red particles after a duration T. Thus $G_\theta(\phi, T, B) = x(T)$, with $x(t)$ being solution of the following Cauchy problem:

$$\begin{cases} \frac{dN}{dt} & = Ng(x, N) \\ \frac{dx}{dt} & = x(1-x)h(x, N) \\ N(0) & = B \\ x(0) & = \phi \end{cases} \tag{3}$$

B.2 Relation with the stochastic evolutionary model

As explained in the main text, the growth function $G(\phi)$ defines the recurrence relation between the colour of the newborn offspring and its colour at adulthood. If the reproduction process entails no stochasticity, the latter also defines the composition of collectives at the next generation. As a consequence, the iterative application of G approximates (though with some bias) the change in time of the adult colour when a population with a given, fixed, set of parameters is transferred across collective generations.

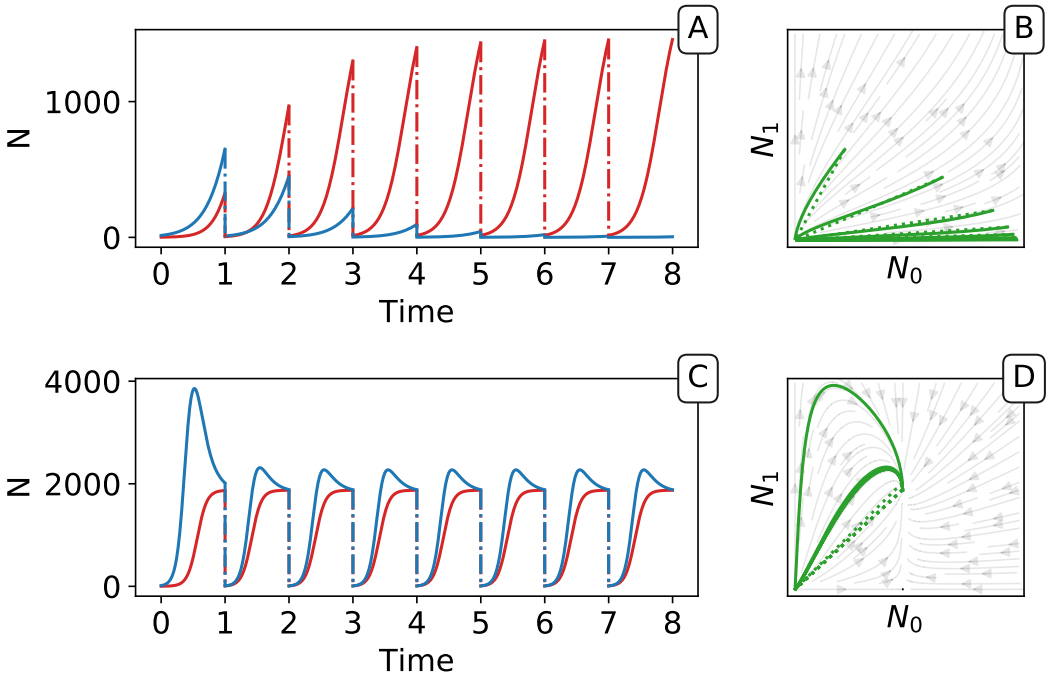

Figure 2: **Piecewise continuous trajectory**. Iterating the deterministic model yield a piecewise continuous trajectory in the N_0, N_1 space. The growth phase (continuous lines) alternate with the dilution (dotted). (A,B) uses traits from generation 3 and (C,D) uses traits from generation $9,000$ of the main simulation with selection 2. Successive adult states can be computed using the G function as a recurrence (see Figure 5 in the main text).

The fixed points of this discrete-time system allow us to understand and classify the behaviours observed along stochastic evolutionary trajectories. When mutation rate of particle traits is sufficiently small and growth rates are not vanishing, collectives approach such fixed points in a few collective generations by iteration of the G function (Figure 5). The evolutionary trajectory can thus be seen as a succession of fixed points of G. The surface of the fixed points of G as a function of the particle parameters can be computed numerically, as well as its dependence on the collective generation duration T and bottleneck size B. A small number of qualitatively different configurations are possible for the fixed points (illustrated in Appendix B Figure 4 1-4). In particular, the case in which G possesses an internal fixed point of value $\phi = \phi^*$ constitutes the optimal solution to constant selection for collective colour, in that it ensures the highest degree of colour reproducibility, on average, across collective generations.

The parameter values that separate regions with qualitatively different fixed points correspond to transcritical bifurcations, where one of the monochromatic fixed points changes its stability. These lines can be analytically computed, thus allowing to generalize the conclusions drawn from analysing the representative trajectory of Figure 2. In the following, we detail the analysis of how the fixed points of the G function depend on the particle-level and collective parameters.

It is worth stressing here that the deterministic model provides a good quantitative approximation of the system with particle-level and collective-level stochasticity only as far as fluctuations at both levels are small. This is the case if populations of particles are large (as for instance in the case of bacterial populations) and if mutations of particle traits are rare and of small magnitude. However, in all the numerical simulations we performed, the conclusions drawn from its analysis kept holding qualitatively also in the case of sizeable fluctuations.

B.3 Fixed Points of the G function and their stability

In this paragraph, we list the key properties of the G function, determining how the asymptotic collective colour depends on the particle and collective parameters. Proofs of the propositions are provided in the following paragraph.

Proposition 1 (Fixed points of G)**.** *Let $\theta \in E$ be a set of particle traits $T \in \mathbb{R}_+^*$ the duration of the growth phase and $B \in \mathbb{R}_+^*$ the bottleneck size.*

Then, $\phi = 0$ and $\phi = 1$ are fixed point of G_θ $\forall\theta$: $G_\theta(0, T, B) = 0$, and $G_\theta(1, T, B) = 1$.

Moreover, if the stability with respect to ϕ of 0 and 1 is the same, G_θ has an odd number of fixed points in $\phi \in (0, 1)$.

The stability of the monochromatic fixed points with respect to the fraction ϕ of red particles has no general analytic expression, but it can be numerically computed. The number and stability of the fixed points as a function of the collective-level parameters B and T is illustrated in Figure 4. Four different cases are considered, corresponding to the four qualitatively different outcomes of particle-level ecology (competitive exclusion by one or the other type, bistability, coexistence).

The fixed points can nonetheless be calculated in certain limit cases, corresponding to parameter values such that within-collective particle dynamics is exponential or saturating.

Proposition 2 (Quasi-exponential growth)**.** *When T is close to 0 and $Ba_{max} \ll 1$ with $a_{max} = \max_{ij} a_{ij}$ the highest element of the competition matrix A, then G_θ has only two fixed points $\phi = 0$ and $\phi = 1$.*

Moreover, the monochromatic fixed point $\phi = 1$ corresponding to a population completely composed of the (faster) red type of particle is stable, whereas the fixed point $\phi = 0$ corresponding to a population composed of the slow growing type of particle is unstable.

Proposition 3 (Saturating growth)**.** *When T tends to ∞ the fixed points ϕ^* of G and their stability correspond to the equilibria x^* of Equation 1. The following Table 3 lists these equilibria and their stability range.*

	Red alone	*Blue alone*	*Coexistence*
Equilibrium x^*	1	0	$\frac{a_{11}-a_{01}}{Tr(A)-CoTr(A)}$
Stability range	$a_{00} < a_{10}$	$a_{11} < a_{01}$	$a_{11} > a_{01}$ *and* $a_{00} > a_{10}$

Here $Tr(A) := a_{00} + a_{11}$ is the sum of the diagonal (or trace) of A, and $CoTr(A) := a_{10} + a_{01}$ designates the sum of the anti-diagonal elements of A.

By linearising the system in the proximity of the fixed points, it is possible to find exactly the bifurcation parameters where one equilibrium changes stability, thus the limit of the region where exists an interior fixed point x^*. Since the particle-level traits change during an evolutionary trajectory, we focus here on the bifurcation values in the space of the collective parameters T and B. These values delimit the region (see Figure 7) where there exists an internal fixed point.

Even when such fixed point is different from the optimal (selected) value ϕ^*, it can provide a starting point allowing evolution to optimize collective colour. In the stochastic system, extinction of one of the two colours of particles happens instead very rapidly when the monochromatic fixed points are stable.

Proposition 4 (Bifurcations of the monochromatic fixed points of G)**.** *The stability of* 0 *changes at* (T_B^*, B_B^*) *and the stability of* 1 *at* (T_R^*, B_R^*) *such that:*

$$B_R^* = \frac{e^{-\alpha_1 T_R^*} - e^{r_0 T_R^*}}{a_{00}(1 - e^{-\alpha_1 T_R^*})} \qquad \text{with } \alpha_1 = r_0 r_1 \frac{a_{00} - a_{10}}{r_0 a_{00} - r_1 a_{10}} \tag{4}$$

$$B_B^* = \frac{e^{-\alpha_0 T_B^*} - e^{r_1 T_B^*}}{a_{11}(1 - e^{-\alpha_0 T_B^*})} \qquad \text{with } \alpha_0 = r_0 r_1 \frac{a_{11} - a_{01}}{r_1 a_{11} - r_0 a_{01}} \tag{5}$$

These results allow us in particular to understand the interplay between time scales of particle-level ecology and of collective reproduction, whose relationship changes along an evolutionary trajectory. Appendix B Figure 3 illustrates the change of the fixed point of G with the collective generation duration T for typical particle traits in the four different parameter regions considered in Figure 7 A-D. Of particular relevance for understanding the stochastic trajectory illustrated in Figure 2 is panel D.

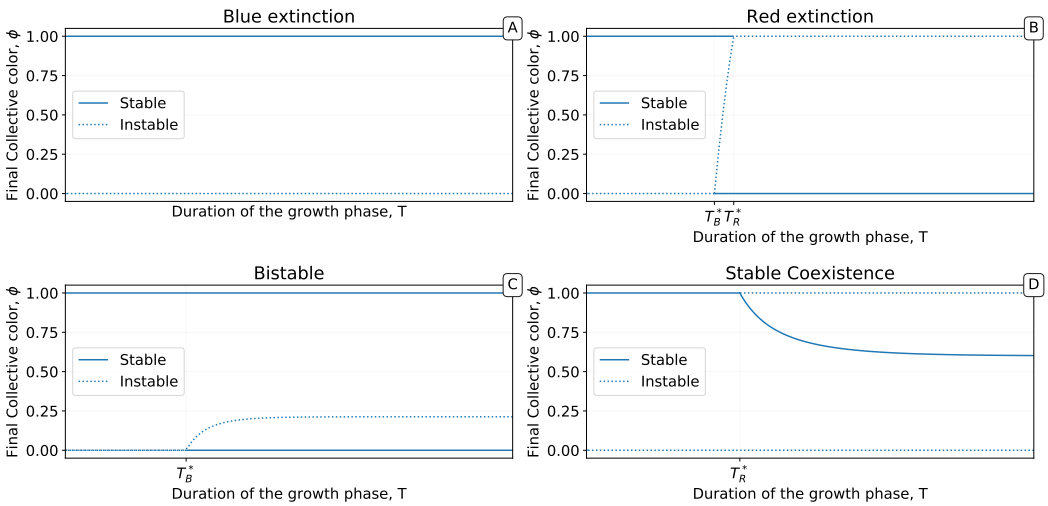

Figure 3: **Bifurcation diagrams showing the position and stability of the fixed points of G as a function of the collective generation duration T.** A-D particle traits are representative of the scenarios illustrated in Figure 7 A-D. Of particular interest is the case illustrated in panel D, where the G function acquires – for a sufficiently large separation between the particle maximum division time and the collective generation time – an internal fixed point.

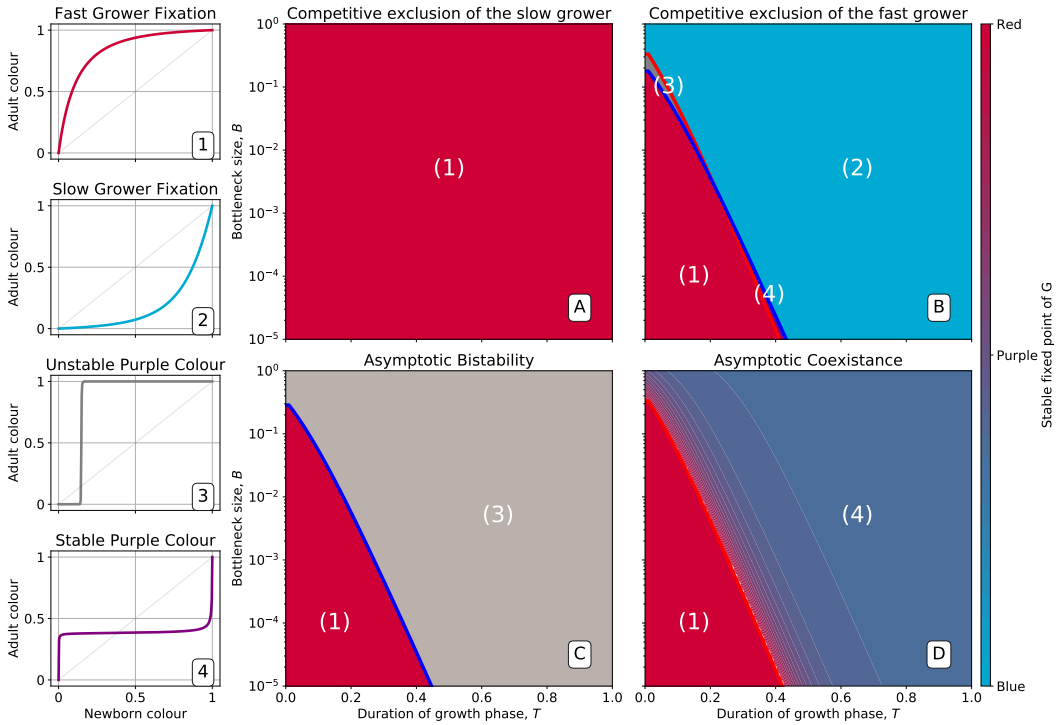

Figure 4: **Qualitative behaviours of the growth function G.** Panels 1-4 represent the possible qualitative shapes, differing in the position and stability of the fixed points, of the growth function G (main text and Appendix B) that approximates the within-collective particle dynamics (orange line in Figure 5). 1) 1 is the only stable fixed point (figure 5A), and iteration of the red G function leads to fixation of the red particles. 2) 0 is the only stable fixed point, and iteration of the blue G function leads to fixation of the blue particles. 3) 0 and 1 are two stable fixed points, and iteration of the gray G function leads to fixation of either red or blue particles depending on the initial conditions. 4) 0 and 1 are unstable and there is a stable fixed point between 0 and 1, and iteration of the gray G function leads to coexistence of both particle types. Panels A-D show how, when red particles are the fast growers ($r_0 > r_1$), the shape of G and the position of its fixed points depend on the collective-level parameters B (bottleneck size) and T (growth phase duration). Particle interaction traits generically belong to one of the four intervals A) $a_{01} < a_{11}$ and $a_{00} < a_{10}$; B) $a_{11} < a_{01}$ and $a_{10} < a_{00}$; C) $a_{11} < a_{01}$ and $a_{00} < a_{10}$; D) $a_{01} < a_{11}$ and $a_{10} < a_{00}$ (nature of the corresponding ecological equilibria is indicated in the titles of the panels). Lines represent the limit of the region of stability of the fixed point of G, as derived by Proposition 4: blue lines for the "all blue" state 0 and red lines for the "all red" state 1.

When the time scale of exponential particle growth is comparable to T, (such as at the beginning of the evolutionary trajectory displayed in Figure 2) Proposition 2 indicates that the system is expected to converge to an all-red solution ($\phi = 1$ is the only stable equilibrium). However, while this fast dynamics occurs, the growth rates have the time to mutate. Selection during the exponential phase generically favours mutants that grow faster, with the side effect that particle populations achieve earlier high-density conditions, where net growth is also influenced by the interaction traits. The system effectively behaves as if T was larger, and interaction traits may be selected.

When the time scale of collective reproduction is sufficiently slow with respect to the intra-collective dynamics, the system will have crossed the bifurcation point T_R^* (Proposition 4), so that the function G now has an internal fixed point (Figure 6). In the stochastic simulations, this means that more and more collectives are reproducibly found close to the optimal colour. It takes a relatively short time to adjust the particle traits so that the fixed point is close to the optimum ϕ^*. In this case, the deterministic approximation produces a close to perfect inheritance of the collective colour. However, fluctuations in particle numbers and in composition at birth still result in a large variance of colours among collectives in the stochastic system.

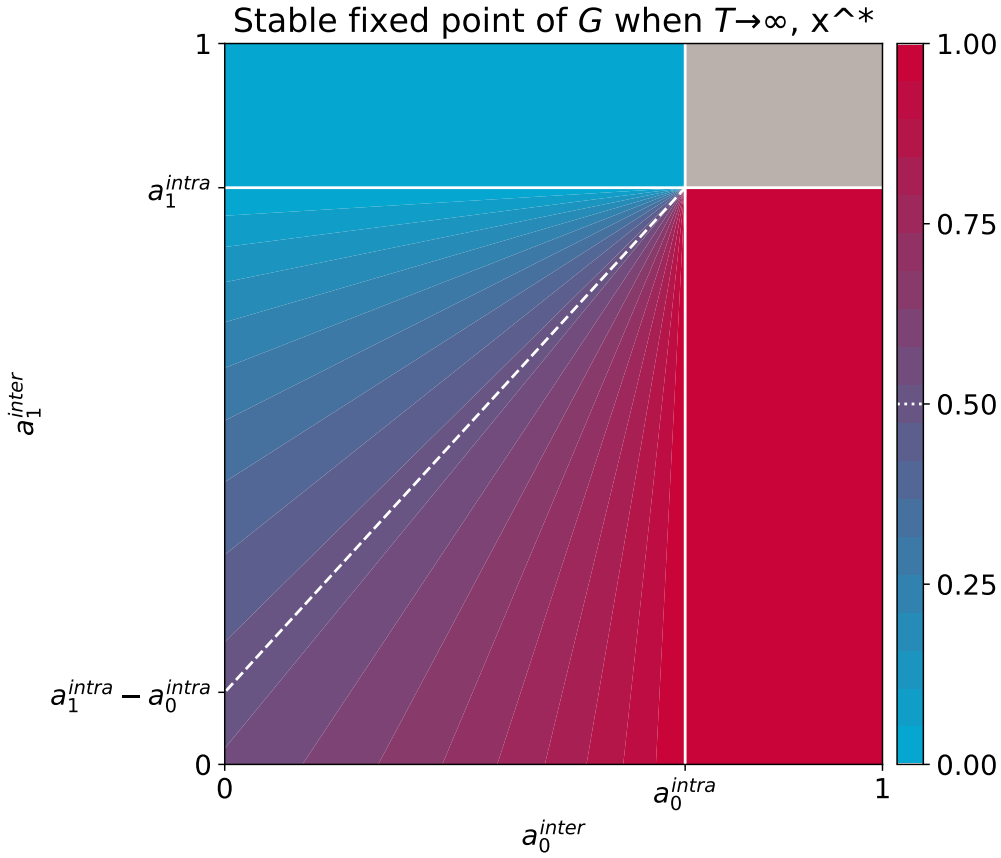

Figure 5: **Stable Fixed point of G as a function of inter-colour competition traits in saturating growth**. This illustrate the results from proposition 3, when $r >> \frac{1}{T}$. $a_{00} = 0.7$ and $a_{11} = 0.8$. The grey area indicates bistability.

Here starts the last and slowest phase of the evolutionary trajectory, that results in colour variance reduction through improvement of the particle ability to correct variations in colour. This is achieved by attaining the particle ecological equilibrium faster, so that fluctuations are more efficiently dampened by the demographic dynamics. As a consequence, the conditions described by Proposition 3 will be met, and this allows to identify, by setting $x^* = \phi^*$, a surface in parameter space containing evolutionary equilibria. Interaction parameters ensuring optimality in the deterministic system thus satisfy the following relationship (growth parameters are in this case $r >> 1/T$):

$$a_{00} - a_{10} + \left(1 - \frac{1}{\hat{x}}\right)(a_{11} - a_{01}) = 0.$$

This relation identifies the white dotted line in Appendix B Figure 5 (and in Figure 8B). Once this condition is attained, mutations would cause the deterministic system to move neutrally on the surface. As the stochastic simulation shows, the stochastic system instead keeps evolving directionally so as to reduce phenotypic variance. This is achieved by making G increasingly flatter in the vicinity of the fixed point, so that the target colour is not only more stable, but it is reached in fewer collective generations (Appendix B Figure 6). Interestingly, successive events of mutation and substitution progressively lead to a growing asymmetry in the ecological relationship between the two types of particles: that with smaller carrying capacity (red) becomes insensitive to the other colour; the latter instead experiences competition, so that its growth is curbed and the good proportion of colours is obtained even in situations when it has an initial growth advantage (see Figure 3D).

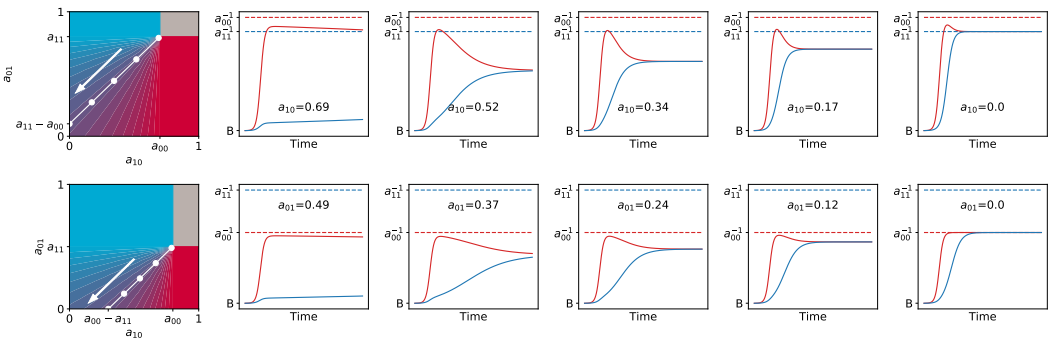

Figure 6: **Asymmetric interaction ensure the fastest convergence toward the equilibrium**. Five particle population dynamics are illustrated for increasingly asymmetric values of (a_{01}, a_{10}) that yields an ecological equilibrium at $x^* = 0.5$ (along white manifold, in the direction of the arrow). Top $(a_00, a_11) = (0.7, 0.8)$, bottom $(a_00, a_11) = (0.8, 0.5)$. In both cases $r_0 = 60, r_1 = 40, T = 1, B = 0.001$.

The growing asymmetry is accompanied by a progressive increase in the attractiveness of the coexistence equilibrium, which results in a faster correction of deviations from the optimal colour. Correspondingly, the growth function G becomes flatter around the fixed point, as illustrated in Figure 6.

B.4 Proofs

In this section we present the proof of propositions 2 - 4 above.

Proof of Proposition 1. In the (N, x) coordinates we have seen that $\frac{df(t)}{dt} = g(x(t), N(t))$ and that $x(t) = 0$ and $x(t) = 1$ are trivial roots of the polynomial g (Equation 2). Hence 0 and 1 are always fixed points of G_θ.

Since g and h (from Equation 2) are polynomials of (N, x), they are smooth (of Differentiability class C_∞) on $\mathbb{R}^2$. Thus the global flow corresponding to the Cauchy problem is also smooth on $\mathbb{R}^2$. G_θ is the partial application of the global flow to the case where $N_0 = B$. Thus, G_θ is continuous on $[0, 1]$.

Moreover, let us suppose that 0 and 1 are both unstable. Then $G'_\theta(0, T) > 1$ and $G'_\theta(1, T) > 1$. As a consequence there is an $\varepsilon \in \mathbb{R}$ such that $G_\theta(\varepsilon) > \varepsilon$ and $G_\theta(1-\varepsilon) < 1-\varepsilon$. Since G_θ is continuous, there is an odd number of $c \in [0, 1]$ such that $G(c) = c$ by virtue of the intermediate value theorem. □

In practice, we never encountered cases when more than one internal fixed point was present.

Proof of Proposition 2. Since the nonlinear terms in Eq. 3 are smaller than $Ba_{\max}$, and this is negligible with respect to 1, it is approximated by its linearization as long as the population size remains close to the bottleneck value. Around $t = 0$, the Cauchy problem can be written as:

$$\begin{cases} \frac{dN_0}{dt} = r_0 Bx \\ \frac{dN_1}{dt} = r_1 B(1-x) \\ N_0(0) = xB \\ N_1(0) = (1-x)B \end{cases} \tag{6}$$

In the (N, x) variables, the total population size grows exponentially and is decoupled from the colour. On the other hand, $x(t)$ follows the logistic differential equation:

$$\frac{dx}{dt} = \frac{d}{dt}\frac{N_0}{N_0 + N_1} = \frac{(r_0 - r_1)B^2 x(1-x)}{B^2} \tag{7}$$

$$= (r_0 - r_1)x(1-x) \tag{8}$$

that can be integrated.

For t sufficiently small for the population to be in exponential growth phase, the growth map G_θ can be approximated by the solution $\tilde{G}_\theta$ of Equation 7:

$$G_\theta(x, t) \approx \frac{1}{1 + \left(\frac{1}{x} - 1\right) e^{-(r_0 - r_1)t}} := \tilde{G}_\theta(x, t) \tag{9}$$

This function is strictly convex (or concave) on $(0, 1)$ depending on the sign of $r_0 - r_1$:

$$\frac{\partial^2 \tilde{G}_\theta(x, T)}{\partial x^2} = \left[1 - e^{(r_0 - r_1)t}\right] \frac{2}{\left(xe^{(r0-r1)t} + 1 - x\right)^3} \tag{10}$$

Since $0 < x < 1$ and $t > 0$, $\frac{\partial^2 \tilde{G}_\theta(x,T)}{\partial x^2}$ is of the same sign as $1 - e^{t(r_0 - r_1)}$, that is strictly positive if $r_1 > r_0$, or strictly negative if $r_0 > r_1$.

Thus, $\tilde{G}$ is strictly convex on $(0,1)$ if $r_1 > r_0$, and strictly concave on $(0,1)$ if $r_0 > r_1$. In the first case, red colour $x = 0$ is an unstable equilibrium and blue colour $x = 1$ a stable one, and vice-versa in the second case. Note that the segment $s = [(0,0),(1,1)]$ is a chord of $\tilde{G}$. Thus the strictly convex (resp. concave) $\tilde{G}$ do not intersect with s except in (0,0), (1,1). □

Proof of Proposition 3. When the collective generation time T is much longer than the demographic time scales, the populations within droplets at the adult stage are well approximated by the equilibrium solution of the Lotka-Volterra Equation 1. Solving simultaneously equations $\frac{dN_0}{dt} = 0$ and $\frac{dN_1}{dt} = 0$ (or equivalently $\frac{dN}{dt} = 0$, $\frac{dx}{dt} = 0$) yields the four equilibria listed in table 1 in both coordinate systems. Linear stability analysis allows one to determine the parameter intervals where these are stable.

Name	Red alone	Blue alone	Coexistance	Extinction
Position in $[N_0, N_1]$	$[\frac{1}{a_{00}}, 0]$	$[0, \frac{1}{a_{11}}]$	$[\frac{a_{11}-a_{01}}{det(A)}, \frac{a_{00}-a_{10}}{det(A)}]$	[0,0]
Position in $[N, f]$	$[\frac{1}{a_{00}}, 1]$	$[\frac{1}{a_{11}}, 0]$	$[\frac{Tr(A)-CoTr(A)}{det(A)}, \frac{a_{11}-a_{01}}{Tr(A)-CoTr(A)}]$	Undefined
Condition for stability	$a_{00} < a_{10}$	$a_{11} < a_{01}$	$a_{11} > a_{01}$ and $a_{00} > a_{10}$	Never

Table 1: **Equilibria of the particle populations and their stability**. Ecological equilibria of the Lotka-Volterra system are listed in the two coordinate systems. Here, Tr(A) and $CoTr(A)$ are defined as in the caption of Table 3.

□

Proof of Proposition 4. We consider the case when the fixed point 0 change stability. The stability of the fixed point 1 can be studied analogously.

We want to find the values of the collective parameters (T, B) where a fixed point with $x = 0$ changes stability (thus undergoing a transcritical bifurcation). The difficulty lies in the fact that one needs to estimate the dynamics of the second variable N in order to study the stability of the 2-D system. Luckily, this can be done in the limit when the collective contains almost exclusively particles of one single colour (in this case, blue).

Total population size is in this case decoupled from colour and Equation 2 can be integrated with initial condition $(N_0 x_0) = (B, 0)$, yielding the following trajectory:

$$\left\{ \tilde{N}(t,B) = \frac{1}{a_{11} - \left(a_{11} - \frac{1}{B}\right) e^{-r_1 t}} \right. \tag{11}$$

As long as x is small, its time derivative is approximated by the non-autonomous system:

$$\frac{dx}{dt} \approx x h(0, \tilde{N}(t,B)) \tag{12}$$

with:

$$h(t,B) = \varepsilon[(r_0 - r_1) + \tilde{N}(t,B)(a_{11} r_1 - a_{01} r_0)]$$

Solving this equation allows to compute the adult colour as a function of the parameters T and B. At the bifurcation point (T^*, B^*) where stability of the 0 fixed point changes,

the newborn colour is the same as adult colour: $x(T^*, B^*) = x(0, B^*)$. (T^*, B^*) are then solutions of the integral equation:

$$
\begin{aligned}
0 =& \int_0^{T^*} h(s, \tilde{N}(s, B^*))ds \\
0 =& (r_0 - r_1) + (a_{11}r_1 - a_{01}r_0) \int_0^{T^*} \tilde{N}(s, B^*)ds \\
0 =& T^* r0 \left(1 - \frac{a_{01}}{a_{11}}\right) + \left(1 - \frac{r_0}{r_1}\frac{a_{01}}{a_{11}}\right) \ln\left(\frac{B^* a_{11} + e^{-r_1 T^*}}{B^* a_{11} + 1}\right)
\end{aligned}
$$

Solving for B^* we get:

$$
B^* = \frac{e^{-\alpha T^*} - e^{r_0 T^*}}{a_{00}(1 - e^{-\alpha T^*})} \tag{13}
$$

With $\alpha = r_0 r_1 \frac{a_{00} - a_{10}}{r_0 a_{00} - r_1 a_{10}}$

Figure 7 shows that this approximation retrieves accurately the numerically computed bifurcation lines.

□